ADDIS ABABA UNIVERSITY

ADDIS ABABA INSTITUTE OF TECHNOLOGY

SCHOOL OF CHEMICAL AND BIO-ENGINEERING

Preparation and Characterization of Activated Carbon from Flower Waste Biomass for Methylene blue Removal

BY: Getu Maru

A Thesis Submitted to Addis Ababa Institute of Technology, School of Chemical and Bio Engineering in Partial Fulfillment of the Requirement for the Degree of Master of Science in Chemical Engineering (Process Engineering)

Addis Ababa, Ethiopia

November, 2019

Addis Ababa University

Addis Ababa Institute of Technology

School Of Chemical and Bio Engineering

Process Engineering Stream

This is to certify that the thesis entitled "**Preparation and Characterization of Activated Carbon from Flower Waste Biomass for Methylene blue Removal**" and submitted in partial fulfillment of the requirements for the degree of Masters of Science (Chemical and Bio Engineering, Process stream) that complies with the regulations of the university and meets with the standard quality.

Approved by Examining Board:

Dr.Abubeker Yimam		
Head of School of Chemical and Bio-Engineering	Signature	Date
Dr. Sintayehu Nibret		
Advisor	Signature	Date
Dr.Abubeker Yimam		
Internal Examiner	Signature	Date
Dr. Beteley Tekola		
External Examiner	Signature	Date

DECLARATION

I declare that this thesis entitled "**Preparation and Characterization of Activated Carbon from Flower Waste Biomass for Methylene blue Removal**" has not been submitted in any form for another degree, diploma or an award at any university or other institution of the tertiary education. I confirm that appropriate credit has been given within this thesis where reference has been made to the work of others and has been duly acknowledged. The work was under the guidance of Dr. Sintayehu N. instructor in Addis Ababa University, School of Chemical and Bio Engineering.

Name: Getu Maru

Signature: _____

Date: _____

ABSTRACT

Activated carbon (AC) can be used as an adsorbent to remove pollutants from waste water streams. 520 kg flower biomass waste is generated daily at a single floriculture industry in Ethiopia. Despite AC has been produced from different lignocellulosic biomass waste, utilizing Flower waste biomass (FWB) as a precursor to produce AC has an advantage of being new raw material, easily available, renewable precursor, and can be a way of reducing environmental pollution. This study presents synthesis of AC from FWB by chemical activation method using $ZnCl_2$ and removal of methylene blue (MB) using the as-prepared AC. The parameters in the study were impregnation ratio, carbonization temperature, and carbonization time. Higher BET surface area of 750 $m^2\ g^{-1}$, pore volume of 1.91 $cm^3\ g^{-1}$ and pore diameter of 1.89 nm was obtained at 1:1 impregnation ratio, 500 $^{\circ}C$ carbonization temperature, and 1 hr of carbonization time. Effect of adsorption dosage, PH, initial dye concentration, and contact time on percentage removal of MB were studied. Maximum removal of MB was recorded at 0.05 g adsorbent dosage, 60 min contact time, PH of 10, and initial dye concentration of 10 mg L^{-1}. Kinetics and isotherm studies showed that the adsorption mechanism of MB using FWB based AC follows pseudo second order while both Langmuir and Freundlich model well fitted the adsorption data with maximum removal efficiency of 94.2% and adsorption capacity of 22.39 mg g^{-1}. FWB can be a good precursor for AC production and can be used to remove MB from wastewater.

Key words: Activated carbon, Flower waste biomass, Chemical activation, Surface area, Adsorption

ACKNOWLEDGMENTS

First, I would like to thank the almighty GOD for giving me the strength, patience and wisdom to overcome all the challenges I faced, for his protection and an ever present helps in my entire situation.

I would like to express my deep and sincere gratitude to my advisor Dr. Sintayehu Nibret for his invaluable supervision, inexpressible support, and continuous guidance without which it could have been impossible to complete this thesis work. His unlimited encouragements, motivation and suggestions have been always a source of inspiration and energy for me. He was much more than an advisor for me.

I would like to thank Bezawit Tatek Shiferraw, Phd candidate at Department of Energy Science and Technology at Myongji University, Republic of Korea, for her best effort in measuring BET surface area of the as-prepared samples.

I would like to thank all staff members working at college of Chemical and Bio-Engineering, Addis Ababa Science and Technology University, Ethiopia for their valuable support through offering me the opportunity of performing experimental works at their research and food laboratory and providing necessary facilities. I acknowledge staff of School of Chemical and Bio-Engineering, Addis Ababa Institute of Technology, Addis Ababa University, Ethiopia and all my colleagues for their support during the thesis work. I must acknowledge Ethiopassion Plc. for providing me the raw material.

Last but not least. My deepest thanks and love goes to my families for their faithful encouragement and invaluable support during my life. I am grateful to Zemzem Ali for her continuous encouragement until the completion of this thesis. Thanks to their endless kind support to reach at this level.

TABLE OF CONTENTS

List of Tables

List of Figures

List of Acronyms

FWB	Flower waste biomass
^oC	Degree Celsius
AC	Activated carbon
MB	Methylene Blue
g	Gram
hr	Hour
t	Time
min	Minute
cm^3	Cubic centimeter
C_o	Initial concentration of MB
C_e	Equilibrium concentration of methylene blue
q_e	Equilibrium adsorbed Amount of methylene blue
mg g^{-1}	Milligram per gram
mg L^{-1}	Milligram per litter
PH	Negative logarithm of concentration of hydrogen ion
K_1	Pseudo-first order rate constant
K_2	Pseudo-second order rate constant
K_L	Langmuir isotherm constant
K_F	Freundlich isotherm constant
R_L	Dimensionless separation factor
R^2	Correlation coefficient
$ZnCl_2$	Zinc chloride
I.R	Impregnation ratio
nm	Nano-meter
mg	Milligram
H_3PO_4	Phosphoric acid
H_2SO_4	Sulfuric acid
NaOH	Sodium hydroxide
HCL	Hydrochloric acid

KOH	Potassium hydroxide
CO_2	Carbon dioxide
N_2	Nitrogen gas
CHNS	Carbon Hydrogen Nitrogen and Sulfur
mm	Millimeter
BET	Brunauer-Emmett-Teller
LSP	lapsi seed stone
Plc	Private limited company
SEM	Scanning electron microscope
EDS	Energy dispersive X-ray spectroscopy
RSM	Response surface methodology
BBD	Box-Behnken Design
ANOVA	Analysis of variance

1. INTRODUCTION

1.1 Background

Currently, with the development of dye industry the associated wastewater pollution has drawn increasing attention (Liu et al., 2014). Dyes can be defined as a colored, ionizing and aromatic organic compound which show affinity towards the substrate to which it is being applied (Singh, Kumar, & Srivastava, 2017) ;organic compounds that provide bright and lasting color to other substances (Chincholi M., Sagwekar P., Nagaria C., 2014). They are toxic, carcinogenic in nature and their addition into nearby streams and rivers contaminates water and greatly upsets the biological activities of aquatic life (Chequer D. & Oliveira R. 2019). Methylene blue is a cationic polar organic water soluble dye and is one of the most widely used dyes in various industries such as textiles and dyeing which, due to toxicity, causes several environmental problems such as; reduction in diffusion of light ,cause respiratory disease and eye damage ((Abbasi & Asgari, 2018) (Corda & Kini, 2018).

There are Different treatment techniques, such as reverse osmosis, precipitation, coagulation, filtration, chemical oxidation, electrochemical methods, aerobic and anaerobic microbial degradation, membrane separation, ion exchange, biological techniques and adsorption are used to remove these dyes and other hazardous materials from wastewater streams prior to release to the environment (Gonawala & Mehta, 2014); (Corda & Kini, 2018). Adsorption using highly porous and larger surface area adsorbent is of the recent methods used for treatment of waste water streams because it is efficient, economical (Chincholi M., Sagwekar P., Nagaria C., 2014), user-friendly, ability to elimination a wide range of toxic pollutants, relatively simple technologies and ease of operation, low generation of residues and the adsorbent used may be regenerated and reused as compared to other existing methods (Corda & Kini, 2018); (Abbasi & Asgari, 2018).

Activated carbon is known for its high absorptivity due to larger internal surface area, higher degree of porosity, large adsorption capacity, fast adsorption kinetics, and relative ease of regeneration, higher electrical conductivity, good thermal stability that makes it to be widely used in the recent years. Hence, owing to its vast applications, the demand for activated carbon in world market is increasing through time due to industrialization and various economic activities. However, commercial activated carbon is particularly produced from coal, lignite, peat, petroleum residue

and wood which are very expensive and exhaustible making AC production costly as explained by(Abdulsalam, Mulopo, Oboirien, Bada, & Falcon, 2019). Because of this in recent years, many researchers have been using agricultural wastes as precursors for the production of activated carbon based on four main reasons; renewable source, inexpensive, readily available and environmental friendly. It is possible to get a BET surface areas ranging between 250 and 2410 $m^2 g^{-1}$, and pore volumes of 0.022 and 91.4 cm^3g^{-1} during production of activated carbon from different agricultural residues under certain process conditions (Ioannidou & Zabaniotou, 2007).

Activated carbon from agricultural wastes can be derived using two main unit processes; carbonization and activation. Carbonization is a thermochemical conversion of organic biomass into gaseous or/and liquid fuels at high temperature in the absence of oxygen and without addition of chemical agents during which most of the non-carbon elements (hydrogen, oxygen, traces of sulfur and nitrogen) are removed in a gaseous form by pyrolytic decomposition. Activation is the process of activating the surface of char produced from carbonization in order to increase its surface area and pore volume which are responsible for adsorptive capability. There are two types of activations: physical (thermal) and chemical. Physical activation is the physical activation process involves the carbonization of the raw material followed by activation of the char produced using steam or CO_2 (M.A. Tadda, A. Ahsan, A. Shitu, M. ElSergany, T. Arunkumar, Bipin Jose, M. Abdur Razzaque et al., 2016). In contrast, chemical activation involves the use of chemical reagents such as KOH, NaOH, $ZnCl_2$ and H_3PO_4 (Abdulsalam et al., 2019).

Floriculture industry is a new fast growing export business in Ethiopia concerned with commercial production, marketing, and sale of bedding plants, cut flowers, potted flowering plants, foliage plants, flower arrangements, and noncommercial home gardening. Ethiopia is the second largest flower exporter in Africa, with over 100 flower growers on 1700 hectares (In & Tilahun Advisor, 2013). Flower waste biomass (cutoff crop parts; stem, damaged flower and leaves) is generated in a higher quantity at floriculture industries (Kassa, 2017).

1.2 Problem Statement

Recently, various toxic chemicals such as micro-pollutants, personal care products, pesticides, textile dyes and inorganic anions have been found at dangerous levels in surface and ground waters throughout the world. Contamination of water is one of the most challenging global issues because it is a huge threat to both human health and the existence of symbiotic relationship between human and environment. Textile dyeing is becoming a major industry in Ethiopia as many industrial parks are being constructed. Different steps in the dyeing and finishing processes produces large volumes of wastewater with great chemical complexity and diversity which are not adequately treated in conventional wastewater treatment Plant. MB is one of the common dye released from textile wastewater streams. As a consequence of those significant impacts it is absolutely necessary to have economically viable and environmentally friendly system for the removal of pollutants from wastewaters streams to safeguard the environment.

Adsorption of dyes using carbonaceous materials such as AC is the most economical and effective method for removal of dyes as a remedy to clean the water prior to its release to the environment. However, using AC to treat wastewater in Ethiopia has two major challenges. First, Ethiopia entirely depends on imports to fulfill its AC demand. According to the data from Ethiopian Revenue and Customs Authority, around 73.5 ton of AC was imported in 2011. Second, Ethiopia's domestic market for AC is increasing due to rapid growth of several end user industries and country's strategic plan to comply with green development strategy. As a result, exploring locally available raw materials for AC production is vital.

Significant amount of Flower waste biomass (cutoff parts such as stem, leaves and damaged flowers) is generated at the flower farms in Ethiopia and this FWB can be taken as a good precursor for the production of activated carbon. For example, Ethiopassion Flower Farm alone generates approximately 520kg/day flower based green waste and there are more than 100 flower grower industries in Ethiopia. In addition, unknown amount of flower waste is generated after different events and simply disposed to the environment. As a result, FWB is highly available potential raw material and can be a good opportunity to produce AC from the cutoff parts and flower petals. Thus, this study is a new effective solid waste management method by producing AC from FWB which can be used in removal of contaminants in wastewater streams. In addition, producing AC from FWB can be considered as an import substitution.

1.3 Objectives

1.3.1 General Objective

The main objective of this study is to prepare activated carbon from flower waste biomass and its application in removal of Methylene blue.

1.3.2 Specific Objectives

The specific objectives are:

- Identifying and characterization of floriculture wastes that can be used as a precursor for AC production
- Investigating effect of Preparation variables (impregnation ratio, activation time and temperature) on BET surface area
- Characterizing textural properties (BET surface area and iodine number) and morphological properties(SEM and EDS) of the AC produced from FWB by $ZnCl_2$ activation
- Investigating adsorption of MB using (pseudo first & pseudo second order) kinetic models and (Langmuir, Freundlich and Temkin) isotherm models.

1.4 Significance of the Study

This study has a significance in introducing an alternative raw material, FWB being available, largely unused, non-food competitive and low cost agricultural waste for activated carbon production. The study can be used as a starting material for further research studies by provide information about significant wastes produced from floriculture industries in Ethiopia. Hence, it provides a means to exploit and manage local resources. It also provides fundamental information for policy makers and AC manufacturers on the potential of FWB as a raw material for AC preparation.

1.5 Scope of the Study

This study mainly focuses on the preparation of activated carbon from FWB at different experimental conditions (activating agent to precursor ratio, activation temperature and activation time), and characterization of the produced activated carbon (proximate, ultimate and surface properties). Finally, the study is being completed by performing adsorption test for MB removal using AC with the highest surface area.

2 LITERATURE REVIEW

2.1 Activated carbon production

2.1.1 Raw materials for activated carbon production

The porous structure and chemical nature of an activated carbon is a function of the raw materials used in its preparation and the activation method. This is the reason why surface area or pore volume of activated carbons can vary widely from one kind to another. It has been reviewed by (González-García, 2018) any cheap material, with a high carbon content and low inorganics can be used as a raw material for the production of AC. It was reported as the use of lignocellulosic resources and waste biomass has had an important impulse because the precursors are diverse, abundant, and renewable, the synthesis process is relatively simple due to the high reactivity of the biomass; and it contributes to decreasing costs of waste disposal to the environment.

Generally; carbon content, inorganic content, volatile content, availability, Potential extent of activation, cost of material are factors to be considered during selection of raw material for activated carbon production. Wood and coconut shells are the most common precursors for the large scale synthesis of activated carbon, yielding to a global production of more than 300,000 tons/year (Ioannidou & Zabaniotou, 2007) (Schröder, Thomauske, Weber, Hornung, & Tumiatti, 2007). However, the problem is high cost of those precursors which leads to finding of an alternative raw material.

In fact, Different literatures indicates that there have been many attempts to obtain low-cost AC or adsorbent from agricultural wastes such as peanut shell (Zhang et al., 2015), olive stones (Berrios, Martín, & Martín, 2012), *Jatropha curcas* fruit shell (Tongpoothorn et al., 2011), cotton waste (Tian et al., 2019) ; (Deng, Yang, Tao, & Dai, 2009); orange peel (Khaled et al., 2009) tomato stem (Fu et al., 2017), grape industrial processing waste (Sayılı, Güzel, & Önal, 2015), Coffee husk and extract residue, (Oliveira et al., 2009). oil palm wood and shell (Ahmad et al., 2007) sunflower and peanut shell, cocoa shells (Pereira et al., 2014), waste tea(Gurten, Ozmak, Yagmur, & Aktas, 2012), bamboo scaffolding (Mui et al., 2010) and avocado kernel seeds (Rodrigues, da Silva, Alvarez-Mendes, Coutinho, & Thim, 2011) which are characterized by their renewability, high mechanical strength, cheapness, abundance, as well as low as contents.. It can be summarized that lignocellulosic biomass components such as: stem, shells, peels, seed, fiber, wood and others can be considered as a suitable starting materials for activated carbon production.

2.1.2 Material pretreatment

There is usually a pretreatment stage prior to the actual AC production process; collection, washing, drying, size reduction and sieving of the raw material. Size reduction to an appropriate Particle size is important for easy of handling and, suitability in mixing with an activating agent during impregnation, but it can also affect the properties of the activated carbon to be produced. Most researchers use the raw materials in a 1–2 mm size, which has been found to be suitable for further processing and activation of the material.(Kumar & Jena, 2015); (Sayğılı & Güzel, 2018) while others either use a smaller particle size [(Ozdemir et al., 2014); (Sayğılı & Güzel, 2018)] or use the raw material in its original form. Evidences show that smaller particle size enhance the surface area of the activated carbon which makes it better for adsorption.

An early research by (Şentorun-Shalaby, Uçak-Astarlioğlu, Artok, & Sarici, 2006) has been conducted on preparation of activated carbon from apricot stone and examined the effect of particle size of apricot stones on the properties of the carbon produced. Four particle size ranges (0.85–1.70 mm, 1.70–3.35 mm, 3.35–4.00 mm and 1.00–3.35mm) were examined and results showed that activated carbon produced from the smallest particle size of apricot stone had low solid yield (4.7%) but highest in surface area (1157 m^2 g^{-1}) and highest pore volume (0.39 cm3 /g) as compared to that of AC from the larger particle size apricot stone.

Another recent research has been done by (Abdulsalam et al., 2019) on Experimental evaluation of activated carbon derived from South Africa discard coal for natural gas storage to see the effect of particle size (0.15–0.25 mm, 0.25–0.5 mm, 0.5–1 mm) on adsorptive properties of activated carbon and results showed that larger particle size end up with a decrease in surface area and pore volume of the activated carbon produced. About 35% decrease in surface area was observed as the particle size increases from 0.15–0.25 mm to 0.25–0.5 mm and 51% further decrease was observed as the size is increased to 0.5–1 mm. The same observation hold for the pore volume as 37% and 46% decrease respectively was observed. But the raw material used is coal so it is of high mechanical strength which allows to enough solid yield even for minimum particle size of the starting material. This might not be true for using minimum particle size lignocellulosic biomass precursors because of low solid yield during the AC production. In general it can be concluded that the coarser the particles the smaller the resulting surface areas of the carbons.

2.1.3 Methods of AC production

Generally there are two methods of activation: physical activation and chemical activation(Varil et al., 2017). In physical activation, the precursor is developed into activated carbons using gases. The raw material (biomass precursor) is pyrolyzed at high temperatures in absence of air followed by activation with oxidizing agents (carbon dioxide, oxygen, or steam) at high pressure and temperature (Chang et al., 2015). In chemical activation, raw material is first mixed with activating agent at specific ratios and then the impregnated raw material is being carbonized at lower temperatures (comparatively lower than physical carbonization(González-García, 2018). González-García, 2018 reviewed synthesis and carbonization techniques for activated carbon production and suggested that Chemical activation is preferred over physical activation because it requires lower temperatures, shorter time for activating the material and higher AC yield.

2.1.3.1 Physical activation

As illustrated by (Paraskeva, Kalderis, & Diamadopoulos, 2008). Physical activation is a two stage process involving carbonization of the material at high temperatures under an inert atmosphere (N_2, Argon) at first in which the material decomposes into fractions: chars, tars and gases followed by the actual activation stage where the charred material comes into contact with the activating agent (steam, CO_2, air) under heating and for a specific retention time. The activating agents are responsible for extracting carbon atoms from the structure of the char through oxidization which leads to the formation of pores. Several research works have proven that a number of lignocellulosic biomass products can be converted in to activated carbons of desired characteristics using physical activation method.

Şentorun-Shalaby et al., 2006 used apricot stone for activated carbon production at 800 ^{O}C and 4hr using steam as an activating agent. Under those conditions surface area of 1092m^2g^{-1} has been reported. AC production from bamboo by steam activation at 850^{o}C were studied by(Ma, Zhang, Zhu, Yu, & Liu, 2014) and results showed an achievement of higher surface area (2024 m^2g^{-1}) and pore volume(0.569 cm^3g^{-1}). (Sivaraj, Rajendran, & Gunalan, 2010) tested the production of activated carbon by physical activation with air from Parthenium hysterphorous (Linn) and resulted in 498m^2/g of surface area at 600^{o}C and 1hr. (Baseri, Palanisamy, & Sivakumar, 2012) studied the preparation and characterization of AC from Thevetia peruviana through carbonization

at 400 ^{o}C and activation with air at 800 ^{o}C for 10 min. surface area of 329.7 m^2g^{-1} has been reported from the result.

Selvaraju & Bakar, 2017 prepared activated carbon from Artocarpus integer fruit processing waste through pyrolysis at 700 ^{o}C and activation step with steam in a temperature range of 550 ^{o}C -750^{o}C for retention time of 20-50min. maximum iodine adsorption of (1411 mg g^{-1}) was achieved under activation conditions of 750 ^{o}C and 60 min. minimum iodine number approximately (960 mgg^{-1}) were obtained at 550^{o}C. Thus the result showed that iodine number increased as temperature increases. The retention time were also affects the iodine number. As time increases from 20 to 60 min iodine number were also increase. However further increase to 100min results in lower iodine number approximately (400 mg g^{-1}) at 550 ^{o}C of activation temperatures.

Babassu endocarp were used to prepare activated carbons by physical activation via microwave radiation at pyrolysis temperature 600°C and were activated in CO_2 atmosphere at 700, 750 and 800 °C for 30 min. Results obtained show that surface area were in the range of 480 to 543 m^2g^{-1} (Salgado, Abioye, Junoh, Santos, & Ani, 2018). Rezma, Birot, Hafiane, & Deleuze, 2017 studied the preparation of activated carbon from Date palm petioles at pyrolysis temperature of 1000^{o}C under nitrogen flow and then activation at 750, 850 and 900 ^{o}C under CO_2 flow and the resulted activated carbon surface area were in the range of 225 m^2 g^{-1} to 546 m^2 g^{-1}. In all these studies of AC preparation via physical activation the most important parameters examined were activating agent, temperature and retention time. Steam and CO_2 or CO_2 mixtures with N_2 were among the activating agents used in the majority of studies. Generally, it can be seen that physical activation requires high activation temperature and also longer retention period which results in minimum AC yield.

2.1.3.2 Chemical activation

In chemical activation a chemical agent is used prior to activation. The commonly used chemicals include H_2SO_4, H_3PO_4, KOH, NaOH and $ZnCl_2$. The processes involve impregnation of the material with the chosen chemical in solid or liquid form. Such impregnation can take up to 24 h depending on the chemical used, the precursor and the subsequent processes. Apart from temperature and retention time, the ratio of chemical to precursor is of paramount importance. A washing step of the material is also involved either with distilled water or a mild acid, to remove residual chemicals from the material (Paraskeva et al., 2008). Varil et al., 2017 examined the effect

of impregnation ratio and activation temperature on preparation of activated carbon from peat. The material was impregnated with different ratios of $ZnCl_2$ (1/4:1-2:1) under mechanical stirring for impregnation time of 3hr and activated at temperatures ranged from 773 to 1073 K under nitrogen atmosphere for 2hrs. The results showed that at a constant impregnation ratio of 2, increasing activation temperature from 773 K to 873 K leads to increase in surface area of the AC from 511 $m^2 g^{-1}$ to 923 $m^2 g^{-1}$. However, further increasing the activation temperature to 1073 K resulted in decrease of surface area to 790 $m^2 g^{-1}$. Similarly at a constant optimum activation temperature of 873 K, increase of impregnation ratio from ¼ to 1 increased surface area from 341 $m^2 g^{-1}$ to 1361 $m^2 g^{-1}$. The decrease in surface area was attributed to the distraction of micropores.

Guo et al., 2019 impregnated prawn shell with KOH at a ratio of 3:1 under nitrogen environment for 3 hr at activation temperature of 800 ^oC producing activated carbon with surface area of (3160$m^2 g^{-1}$). An early research studied by (Caturla, Molina-Sabio, & Rodríguez-Reinoso, 1991). indicated the impregnation of peach stones with $ZnCl_2$ solution in the ratio ($ZnCl_2$: material) 0.4:1–2.5:1 for impregnation time of 24hr. then it was subjected to be carbonized under nitrogen flow from 500-800^oC producing higher surface area of 3000 $m^2 g^{-1}$. The results from investigation of effect of impregnation ratio showed that an increase of ratio from 0.2:1 to 1:1 increased surface area from 1000 to 2000 $m^2 g^{-1}$ but further increase resulted in decreased surface area at 2.5:1. This was due to the widening of the micropores at increased ratio of $ZnCl_2$ beyond 1:1. Also increasing temperature to 600^oC resulted increased surface area, however further increase in temperature showed decreased surface area.

El-Sayed, Yehia, & Asaad, 2014 studied the assessment of activated carbon preparation from corncob via chemical activation using phosphoric acid. The material was impregnated with H_3PO_4 in a ratio 1:2 and carbonized at 400, 500 and 600 ^oC for constant retention time of 2hr. results showed that surface area of 700 $m^2 g^{-1}$, 633 $m^2 g^{-1}$ and 600 $m^2 g^{-1}$ were achieved at 400, 500 and 600^oC respectively. Saad et al., 2019 experimented with preparation of AC from rice straw via KOH activation. The rice straw was impregnated with KOH by soaking in KOH solution (13 M) with a weight ratio of 1:4 (1 g RSC: 4 mL KOH) for 24 h. The result material was activated at temperatures 650 ^oC, 750 ^oC and 850 ^oC under nitrogen gas flow (100 ml/min) for 2 hr. results obtained showed that rice straw AC exhibited BET surface area ranging from 520 to 1048 $m^2 g^{-1}$. BET surface area of rice straw derived AC increased with increasing activation temperature from

650 to 850 ℃ with minimum (520 $m^2 g^{-1}$) at 650℃ followed by (928 $m^2 g^{-1}$) at 750℃ and highest surface area (1048 $m^2 g^{-1}$) at 850 °C.

Sahira, Mandira, Prasad, & Ram, 2013 examined the effect of different activating agents (KOH, H_2SO4, $FeCl_3$, $MgCl_2$, and $CaCl_2$) on the preparation of activated carbon from lapsi seed stone. Powdered lapsi seed stone were mixed with those activating chemicals and carbonized in a muffle furnace under continuous flow of ultra-pure nitrogen gas (75 ml min^{-1}) at 400 ^oC for 3hr. Highest iodine number of AC were obtained from KOH activation with iodine number (510 mg g^{-1}) and lowest iodine number (330 mg g^{-1}) was obtained from impregnation with $MgCl_2$. 502 mg g^{-1}, 381 mg g^{-1} and 431 mg g^{-1}iodine number were achieved from impregnation of lapsi seed stone with $FeCl_3$, $CaCl_2$ and H_2SO4 respectively. The higher Iodine number of these carbons has been attributed to the presence of large micropore structure which may due to chemisorption taking place in the pores of the carbons during activation and might have resulted in the differences in their reactivity with the different activating agents and the enlargement of their pore structure (Sahira et al., 2013). From similar precursor (lapsi seed stone) (Joshi, 2016) studied the effect of IR (1:0.25, 1: 0.5, 1: 1, 1:2 and 1:4 (LSP: ZnCl2)), activation temperature (300, 400, 600 and 800 ^oC) and activation time (3-6 hr) on AC preparation via $ZnCl_2$ activation under ultra-high pure nitrogen (100ml/min) environment. AC yield were continuously decreased with increase in temperature and increased activation time due to the fact that oxygen and hydrogen from the precursor released in the form of CO, CO_2, and CH_4.

The increase in ZnCl2 /Lapsi seed powder ratio in general increased the iodine and methylene blue number indicating the increase in adsorptive capacity and meso and micro porosities in the resulting activated carbon. On increasing LSP: $ZnCl_2$ equals to 1:1, iodine number and methylene blue number increased only marginally indicating the attainment of equilibrium concentration. Similarly increasing carbonization time from 3hrs to 4hrs there was significant increase in iodine number and methylene blue number and there after the increase is gradual. Likewise increase in iodine number and methylene blue number with increase in carbonization temperature above 400 ^oC is gradual. At 400 ^oC the decomposition of LSP lignocellulosic material is almost complete as evident by the TGA curve (Joshi, 2016). it is understood that IR of 1:1, carbonization temperature of 400oC and carbonization time of 4hr were optimum conditions for the AC preparation from lapsi seed stone with iodine number and methylene blue number of 791 mg g^{-1} and 364 mg g^{-1}

respectively. From this result it can be concluded that $ZnCl_2$ activation resulted in higher iodine number as compared to (KOH, H_2SO4, $FeCl_3$, $MgCl_2$, and $CaCl_2$) activation for AC production from same raw material, lapsi seed stone. Latest research conducted by (Sayğılı & Güzel, 2018) on preparation of activated carbon from novel precursor, carob processing residue to examine the effect of impregnation ratio (1:1, 2:1, 4:1, 6:1 and 8:1;$ZnCl_2$/CR, g/g)), carbonization temperature (400, 500, 600 and 800 ^oC) and contact time(0.5, 1, 2 and 4hr). The process were performed by impregnating dried powdered carob residue with different ratios of $ZnCl_2$ and then carbonization under nitrogen flow for different temperature ranges and carbonization durations. AC from Carob residue without ZnCl2 activation resulted in surface area of 66 $m^2\ g^{-1}$ at carbonization temperature of 500 ^oC.

The effects of IR on the textural properties of the produced ACs were evaluated with the conditions of carbonization temperature of 500 ^oC and carbonization time of 1 h. results showed that surface area of the produced AC increased from (837 to 1641 $m^2\ g^{-1}$) and pore diameter from 2.48 to 5.28 nm, as the impregnation ratio increased from 1:1 to 6:1. However, further increase in IR resulted in decreased surface area and pore diameter. From these results, it is understood that IR significantly affect to porosity. With low IR, due to the effect of $ZnCl_2$, the formation of tar is inhibited and the release of volatiles is promoted, producing more micropores. But at higher IR, the more swelling into impregnated precursor and stronger release of volatiles in the carbonization process will lead to the widening of pores; micropores formed are subsequently converted to mesopores(Sayğılı & Güzel, 2018).

On the other hand the effects of carbonization temperature on textural properties of the produced AC were examined at IR of 6:1 and carbonization time of 1hr. BET surface area, total pore volume and pore diameter of AC were increased from (1014 to 1693 $m^2\ g^{-1}$), (0.633 to 2.655 $cm^3\ g^{-1}$) and (2.5 to 6.7 nm) respectively as carbonization temperature raised from 400 to 600 ^oC and then decreased when temperature was increased above 600 ^oC. The increased in the investigated textural properties of the AC with increase in carbonization temperature were due to the formation of new pores by continual removal of volatile components from pyrolytic decomposition of the raw material up to 600 ^oC. And the decrease in textural properties of the produced AC with further increase in temperature above 600^oC might be resulted from the sintering effect at high

temperature, followed by shrinkage of the char, and realignment of the carbon structure which resulted in reduced pore areas as well as volume(Sayğılı & Güzel, 2018).

Effects of carbonization temperature on AC textural properties were investigated by varying time from (0.5 up to 4 hr) at 600 ºC and IR of 6:1. The results showed that surface area, total pore volume and pore diameter increased from (1601 to 1693 $m^2 g^{-1}$), (2.167 to 2.655 $cm^3 g^{-1}$) and (4.33 to 6.70 nm) with prolonging of carbonization time from (0.5 to 1 h), respectively. But the values of those textural properties declined when the time was higher than 1 h. This decrease was probably because the excessive time lead to the collapse of pores, so the textural properties became smaller (Sayğılı & Güzel, 2018). It can be concluded from the results 600 ºC, 6:1 and 1hr were selected as optimum carbonization time, IR and carbonization time respectively which resulted in best AC properties; highest surface area(1693 $m^2 g^{-1}$), highest total pore volume (2.655 $cm^3 g^{-1}$) and highest pore diameter(6.7 nm).

Sivaraj et al., 2010 studied the preparation of activated carbon from Parthenium hysterophorous (Linn) by physical activation and chemical activation with different chemicals. In physical activation effect of temperature ranging from (400 to 800 ºC) were examined at 1hr.in chemical activation with $ZnCl_2$ the precursor were mixed with $ZnCl_2$ in a ratio ranging from (0.0625 - 1.00) and carbonized at 700 ºC for 1hr. Excess of $ZnCl_2$ on the activated carbon particles were leached out by immersing it in 1M HCl solution for about 24 h (Sivaraj et al., 2010).

During chemical activation with acids, Conc. H_2SO_4, HCl, HNO_3 and H_3PO_4 were mixed with parthenium in a ratio of 1.5:1and carbonized in a muffle furnace for 14hr at 120 ºC. In this study the activating agent for physical activation is not mentioned. As shown from results of physical activation surface area of AC increased from (155.9 to 498.4 $m^2 g^{-1}$) with increase in temperature from 400 to 600 ºC and decreased to 292.45 $m^2 g^{-1}$ during further temperature increment to 800 ºC. Results from acid activation showed that higher surface area (680 $m^2 g^{-1}$) were obtained from H2SO4 activation. While minimum surface area (162.27 $m^2 g^{-1}$) were obtained during HNO_3 activation. From ZnCl2 activation results it is understood that with increase in the impregnation ratio of $ZnCl_2$, the surface area showed an increasing trend from (839.88 $m^2 g^{-1}$-1089.26 $m^2 g^{-1}$). In general from AC prepared by the three activation methods, activation with $ZnCl_2$ produced AC with highest surface area (1089.26 $m^2 g^{-1}$) at IR of 1 and chemical activation resulted in higher surface area AC as compared to physical activation. Ahiduzzaman, 2016 evaluated characteristics

of activated carbon from rice husk using $ZnCl_2$ and H_3PO_4 activation. Results indicated that surface area of AC from $ZnCl_2$ activation was found to be 927 m^2 g^{-1}while surface area of phosphoric acid treated AC was found to be 718 m^2 g^{-1}. From this result it can be understood that $ZnCl_2$ activation resulted in 30% higher surface area than H_3PO_4 activation. This might be due to the capability of zinc chloride to develop smaller size pores in higher degree than phosphoric acid. Generally, from those researches it can be concluded that AC textural properties are functions of impregnation ratio, activation temperature and activation time. Addition of activating chemical develops porosity by means of dehydration and degradation of biomass structure and prevents the formation of tars during carbonization of the raw material leading to increased surface area compared to the AC produced without impregnation.

2.1.4 Batch adsorption

In the recent years researches have been conducted using activated carbon from lignocellulosic materials to study the efficiency of some basic requirements (rate of adsorption and equilibrium data) on adsorption process. Parameters such as initial concentration of adsorbate, pH, and agitation temperature at which experiments are carried out, contact time and adsorbent dosage can be varied to study the effect of adsorption on dyes. El-Sayed et al., 2014 assessed the effect of adsorption parameters on performance of dye removal using three AC samples prepared from corncob. Contact time (10 min to 120 min) study using those AC samples at adsorbent dosage (2 g) and initial dye concentration(25 mg/l) showed that percentage removal increased as contact time increases until equilibrium is reached. The time taken to reach equilibrium was about 45 min for AC-400 and 120 min for AC-500 and AC-600 for the dye concentration used. From this result it can be understood that AC sample with highest surface area reached equilibrium faster. Results from Studies of the effect of initial dye concentration showed that the adsorption capacity of dye increases from 4.9 to 46.0, 4.8 to 39.3 and 4.6 to 37.5 mg/g as the initial dye concentration increases from 5 to 50 mg L^{-1} for AC-400, AC500 and AC-600, respectively. Results from adsorbent dosage study showed that while adsorbent dose increases from 1 to 5 g, percentage of dye removal increased from 96.2% to 99.6%, 98.6% to 99.4% and 41.6% to 91.2% at equilibrium time for AC-400, AC-500 and AC-600, respectively. Finally results of PH study using different AC samples indicated that dye adsorbed was higher at higher pH. And the optimum pH was found to be pH higher than 8. Modeling results signified that Adsorption of MB on AC-400 (R^2=0.9868) and AC-500(R^2=0.9810) followed Langmuir isotherm with adsorption capacity of 28.65 and 17.57 mg/g respectively. While Adsorption on AC-600 was better fitted to Freundlich isotherm model

(R^2=0.9823). Rashid, Jawad, Ishak, & Kasim, 2018 studied preparation of activated carbon from coconut leaves via $FeCl_3$ activation and application for MB removal. The effect of the adsorbent dosage (0.02-0.25 g), initial pH (3-11), initial dye concentrations (30-350 mg L^{-1}) and contact time (1-180 min) on the adsorption of MB at 303 K were performed by batch adsorption experiments. From the results it can be understood that amount of MB adsorbed increased from 21.29 to 64.38 mg/g with increase in initial dye concentration from 30 to 350 mg L^{-1} as a result more time is needed to reach equilibrium at higher initial concentration. Also from effect of adsorbent dosage study Percentage removal of MB increased with increase in adsorbent dosage. Highest removal of MB by coconut leave derived AC was recorded at 0.1 g with 74.87% removal but further increase in dosage beyond 0.1 g did not show any obvious changes. Percentage removal increased up to contact time of 60min above which no significant change was observed. And maximum removal of MB were reported at PH of 11. Modeling results of the adsorption data indicated that kinetics was better described by Pseudo-Second Order whereas the isotherm was fitted by Langmuir isotherm at equilibrium with maximum adsorption capacity (q_{max}) of 66.00 mg g^{-1}.

Effect of contact time studied by (Ahiduzzaman, 2016) using two AC samples one activated with zinc chloride and the other activated with phosphoric acid showed that extent of MB removal increased with increase in contact time due to the fact that strong attractive force is created between dye molecule and the adsorbent at longer contact time. The kinetic curve followed power equation with good correlation coefficient of (R^2=0.99) for H3PO4 activation and (R^2=0.96) for $ZnCl_2$ activation. (Alhamed, 2006) studied adsorption of MB and phenol using activated carbon produced from dates' stone by $ZnCl_2$ activation. Adsorption data for MB and phenol were obtained through equilibrating different masses of AC from (0.05-0.5 g) with 25 ml of 1200 mg L^{-1} MB and 250 mg L^{-1} phenol at room temperature with continuous shaking. Under this investigation the effects of activation parameters; IR (0.5:1, 1:1, 1.5:1 and 2:1), carbonization temperature (500, 600 and 700 ^oC) and carbonization time (0.5, 1, 1.5, 2 and 3 hr) on percentage removal of MB and phenol were examined and results showed that for MB adsorption maximum removal percentage(89.9%) and $(q_{max})_{MB}$ 286.3 mg g^{-1} were obtained at carbonization conditions of IR (2), carbonization temperature(500^oC) and carbonization time of 1hr. for phenol adsorption maximum removal (97.1%) and $(q_{max})_{ph}$ 75 mg g^{-1} were obtained at optimal carbonization conditions of IR=0.5, carbonization temperature=700oC and carbonization time of 3 hr.

3 MATERIALS AND METHODS

The experimental works were conducted in the laboratory of Addis Ababa science and Technology University, college of chemical and bio-engineering and Characterizations such as Ultimate analysis of the precursor were performed at leather industry development institute (LIDI) Addis Ababa, Ethiopia. SEM analysis and EDS analysis were done at Myongi University, South Korea.

3.1 Materials

High power electric motor was used to perform size reduction and particle size distribution was performed using sieve. Soaking and mixing was conducted using different sized borosilicate glass beakers. Electronic balance was employed in order to take weight measurements. Subsequent Sample drying and moisture removal was performed using digital electronic oven. PH meter (Schott AG, Mainz, Germany) and conductivity meter was used to perform acidity and/or basicity and conductivity measurements. During AC washing separation of liquid and solid was performed by centrifugation using centrifuge and filtration using filter paper.

Nabertherm GmbH furnace equipped with digital display (bahnhofstr.20, 28865 Lilienthal/Bremen, Germany was used to perform carbonization process using nitrogen gas contained in a nitrogen cylinder aligned with the furnace by a hose. The elemental analysis of FWB was carried out using an elemental analyzer (Elementar/MACRO, Germany) to determine the percentage composition of C, H, O, N, and S. The pore development of the ACs was explored using N_2 adsorption/desorption isotherms at 77 K, employing a surface area analyzer (Quantachrome/autosorb-iQ-2MP, USA).The morphological structures of produced AC were detected using a scanning electron microscope (SEM) and elemental distribution in the AC structure were determined using EDS. Adsorption experiments were performed by using conical flasks through magnetic stirrer and UV- spectrophotometer to determine MB absorbance.

3.2 Chemicals

All chemicals and reagents used in this study were of analytical grades and supplied from (cherkos, A.A, Ethiopia). Preparation and dilution of all working and standard solutions were performed by dissolving appropriate quantity of the required chemicals in distilled water. A stock solutions of zinc chloride at a concentration of 0.37M, 0.7 M and 1.1 M were prepared by dissolving 25, 50 and 75 g solid zinc chloride (Merck, Darmstadt, Germany) in 500 ml volume of distilled water and

was used as an activating agent. A stock methylene blue solution in this study was prepared from MB ($C_{16}H_{18}ClN_3S$ (Germany)) at a concentration of 1000 mg L^{-1} by dissolving 1000 mg of MB in 1000 ml of distilled water. Standard iodine solution was prepared from dissolution of appropriate amount of potassium iodide (produced in India) with deionized water and standardized with sodium thiosulfate (made in India). The PH of solutions were adjusted by 0.1 M HCl and 0.1 M NaOH.

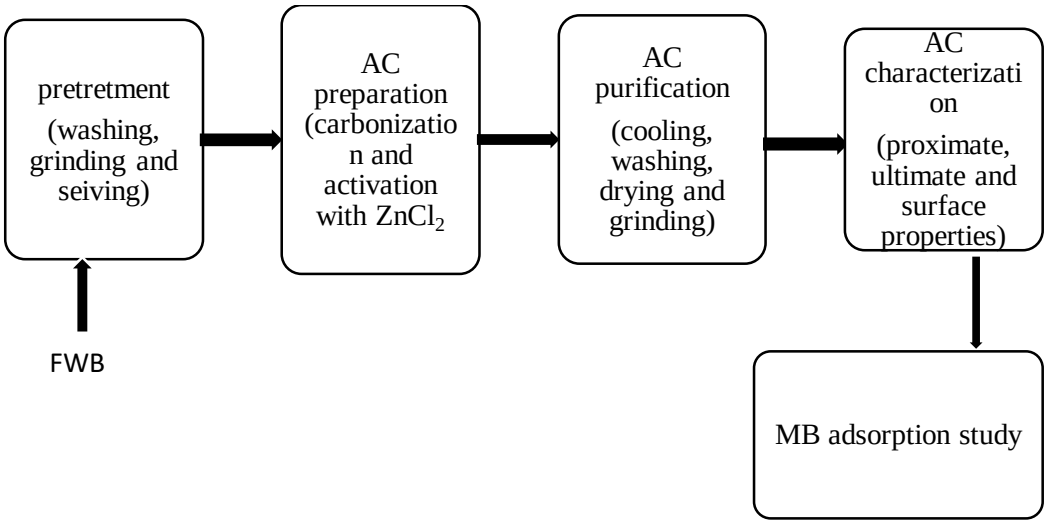

Figure 3.1 Steps involved in the preparation of AC from FWB

3.3 Sample Preparation

Flower waste biomass were collected from Ethiopassion Agro PLC, a floriculture industry in Ethiopia found around Alemgena 20 km from Addis Ababa. The collected FWB sample was washed with distilled water for the removal of dirt and dust particles that may have been presented on their surface. Then it was first sun dried in order to remove moisture content. The dried materials were grounded to a fine powder using high power electrical milling machine and was sieved to get a uniform size distribution between (1- 2 mm). The powdered material were then oven dried for 24 h at 110 ^{0}C for further moisture removal. Proximate analysis (fixed carbon, volatile matters, ash and moisture content) and elemental analysis were analyzed. Finally it was packed by plastic bag and used as a raw material throughout the experiment.

Figure 3.2: Sample preparation procedure, (A) flower, (B) stem

3.4 AC Preparation

50 g FWB sample were impregnated with $ZnCl_2$ solution with three different impregnation ratios of ZnCl2: FWB (w/w, 0.5:1, 1:1 and 1.5:1). The slurry was stirred with magnetic stirrer and simultaneously heated at a temperature of 85^0C to facilitate the impregnation. It was then left for 24hrs with occasional stirring (manual) at room temperature to increase rate of activation. After the impregnation, $ZnCl_2$ treated biomass residues were filtered to remove excess activating agent and dried in an oven at 105 °C for 24 hr. dried mixtures were taken from petri dishes into porcelain crucibles and ready for carbonization. Carbonization were takes placed in a modified furnace at different carbonization temperatures (400, 500 and 600 °C) for different carbonization times (30, 60 and 90 min). The temperature was reached at a rate of approximately 10 °C per min. Nitrogen gas was used to provide an inert atmosphere to prevent oxidation of the samples and to carry volatile matter away from the heating zone. Then, carbonized materials were immediately taken into a desiccator to prevent the contact with oxygen (moisture sacking) and allowed to be cooled to room temperature. Then the weight losses during carbonization were determined and recorded as yield. After the activation and carbonization step, activated carbons obtained were dissolved in 0.1M HCl solutions in order to eliminate contaminants and residual zinc and chloride ions from the pores and surfaces of the AC, and afterwards the activated carbons were washed with hot-distilled water until neutral (desired) pH was achieved. Lastly, activated carbons were dried in an oven at 105 °C for 24hrs, grounded, and packed in closed plastic bags for further use.

3.5 Characterization of FWB and AC

3.5.1 Proximate analysis

As defined by ASTM; D1762-84 (Reapproved 2001), proximate analysis separates the products into four groups: (1) moisture, (2) volatile matter, consisting of gases and vapors driven off during pyrolysis, (3) fixed carbon, the nonvolatile fraction of biomass, and (4) ash, the inorganic residue remaining after combustion. The proximate analysis methods and procedures for FWB and AC are mentioned below.

A. Volatile Matter

The sample was measured and placed in a closed crucible. It was then heated up to 900°C for exactly 7 min in a furnace. The crucible was then cooled in a desiccator and weighed. The weight of the sample before heating and after heating was used to determine the amount of volatile matter present in the sample.

$$\text{volatile matter } (\%) = \frac{W_1 - W_2}{W_1} * 100 \qquad 3.1$$

Where: W1 = weight of dry sample and closed crucible before heating (g); W_2 = weight of dry sample and closed crucible after heating (g).

B. Ash Content

Sample was measured and taken in a crucible. It was then heated to 650 °C for 3hr. During this test the crucible was left open. The heating was done in a muffle furnace. After the required heating, the crucible was cooled in a desiccator and then weighed. In this test, the amount of residual substance is equal to the ash present in the sample.

$$\text{Ash content } (\%) = \frac{W_2}{W_1} * 100 \qquad 3.2$$

Where: W_1 = weight of dry sample before heating (g), W_2 = weight of ash (g).

C. Moisture Content

Sample was measured and taken in a petri dish. It was dispersed nicely on the petri dish. It was then heated at 105°C for 12hr. The petri-dish was left open during the heating process. After heating, the petri-dish was cooled in desiccator and then weighed. This specifies the amount of moisture content present in the sample.

$$\text{Moisture content } (\%) = \frac{W_1 - W_2}{W_1} * 100 \qquad 3.3$$

Where: W_1 = weight of sample and petri dish before drying (gram), W_2 = weight of sample and petri dish after drying (gram).

D. Fixed Carbon Content

The fixed carbon content is determined by subtracting the sum of percentage compositions of moisture content, volatile matter content, and ash content form 100. The value obtained is the amount of fixed carbon present in the sample expressed in percentage.

$$\text{Fixed carbon } (\%) = 100 - (\%\text{ moisture} + \%\text{ volatile matter} + \%\text{ ash}) \quad 3.4$$

3.5.2 Ultimate Analysis of FWB raw material

Elemental composition of the precursor were determined by CHNS/O elemental analyzer which provide a means of determination for percentage composition of carbon, hydrogen, nitrogen and sulphur in organic matrices and other types of materials through complete and instantaneous oxidation of the sample. From these results the oxygen composition is determined by subtracting the sum of Carbon, Hydrogen, Nitrogen, and Sulphur compositions from 100. The Ultimate Analysis was carried out in EA 1112 Flash CHNS/O- analyzer under the condition of carrier gas (He-gas) flow rate of 120 ml/min and oxygen flow rate of 250 ml/min with furnace temperature of 900 °C. The sample, 1gram of FWB (50% flower powder + 50% stem powder) were fed into the analyzer along with excess supply of oxygen. The reaction of oxygen with other elements (namely carbon, hydrogen, nitrogen, and sulphur) present in the sample produces carbon dioxide, water, nitrogen dioxide, and Sulphur dioxide respectively. The combustion products are separated by a chromatographic column and are detected by the thermal conductivity detector (TCD), which gives an output signal proportional to the concentration of the individual components of the mixture. This determines the equivalent compositions of elements in the sample.

3.5.3 AC yield

Activated carbon yield is the ratio of weight of sample after carbonization to the weight before carbonization and it tells us how much of the precursor is changed through the carbonization process. The AC yields were calculated by means of the formula below:

$$\text{yield}(\%) = \frac{W1}{W2} * 100\% \quad 3.5$$

Where; W_1: the weight of FWB used as a starting material for the activated Carbon production (dry basis) and W_2: is the weight of activated Carbon produced via pyrolysis (dry basis).

3.5.4 PH and Conductivity Determination

The pH of the AC was determined by adding 1 g of AC to a 10mL of deionized water for 24 h, and the pH of the mixture was the value of the mixture measured using PH meter. Similarly the conductivity of the activated carbon is the one which is measured by the conductivity meter.

3.5.5 Iodine Number

Iodine number is the most fundamental parameter used to characterize activated carbon performance. It is the standard measure for liquid phase applications and corresponds to the amount of milligrams of iodine adsorbed by one gram of activated carbon when the iodine concentration of the filtrate is 0.02 mol L^{-1}. Iodine number is determined according to the (ASTM D4607-94) method. A standard iodine solution was treated with different activated carbon samples under specified conditions. In the experiment activated carbon sample was treated first with 10mL of 5% HCl and boiled for 30 s and then cooled. Then 100 mL of 0.1 N (0.1 mol L-1) standard iodine solution was added to the mixture and stirred for 30 s. The resulting solution was filtered and 50 mL of the filtrate was treated with 0.1 N (0.1 mol L-1) sodium thiosulfate, using starch as indicator (Debela T., 2016). The iodine number is the X/M value when the residual concentration of iodine in the filtrate is 0.02 N (0.02 mol L-1).

$$X/M = \frac{(N_1 * 126.93 * V_1) - \left[\frac{V_1 + V_{HCl}}{V_F}\right] * (N_{Na_2S_2O_3} * 126.93 * N_{Na_2S_2O_3})}{M_{AC}} \quad 3.6$$

Where: N_1 is the normality of iodine solution, V_1 is the volume of iodine solution added during the titration, V_{HCl} is the volume of 5% HCl mixed with the sample, V_F is the filtrate volume used in titration, $N_{Na2S2O4}$ is the normality of sodium thiosulfate solution used during the titration, $V_{Na2S2O3}$ is the volume of sodium thiosulfate solution consumed during the titration and M_{AC} is the mass of activated carbon used.

3.5.6 Surface Area Analysis

Surface area and pore size of the produced activated carbon were determined using BET surface area analysis method through N_2 gas adsorption at a constant temperature. The method was developed by three persons; Stephen Brunauer, Paul Emmett and Edward Teller in 1938. This method measures surface area and pore size based on gas adsorption on the solid porous material. It gives the surface area by using the adsorption desorption data. From the data one can determine the amount of gas needed to form a monolayer on the surface of the material.

3.5.7 SEM Analysis

The SEM of AC was analyzed using scanning electron microscope to record the surface morphology of the activated carbon. For the SEM image the carbon tape was cut into small pieces and fixed on the disc. Then the upper layer of the disc was removed and very small amount of carbon was placed on the black carbon tape, well fixed just pressing on a clean silicon wafer(Choerospondias & Shrestha, 2015). Finally results were recorded as an image.

3.6 Experimental design

RSM, Box-Behnken experimental design (BBD) with three factors was used for experimental data analysis of AC production process using Design-expert 7.0.0 software. The results obtained from the experiment were analyzed with ANOVA (analysis of variance) to model the relationship between various factors and the responses. Surface area of AC was the response variable. The three variables studied for the preparation of activated carbon were impregnation ratio, activation temperature and activation time as summarized below.

Table 3.1 Independent variables and levels for BBD

Independent variables	Unit	Levels		
		Minimum	Medium	Maximum
Impregnation ratio	_	0.5	1	1.5
Temperature	^{o}C	400	500	600
Time	min	30	60	90

3.7 Adsorption experiment

Adsorptive properties of adsorbent material can be analyzed by means of conducting batch adsorption experiment using standard MB ($C_{16}H_{18}N_3SCl$, AR grade) solution as a test dye molecule. Different factors such as adsorbent dosage, PH, initial dye concentration, contact time, temperature and agitation speed had a significant influence on the adsorption capacity (Gonawala & Mehta, 2014). To investigate the effect of those variables adsorption experiment were conducted in a batch test. 100 mL of MB dye solution of desired concentration was prepared in 250 mL conical flask by suitable dilution of the stock solution and its desired pH was adjusted. Then known amount of AC was added and the resulting mixture were shaken using magnetic stirrer for

predefined time. After stirring, the suspension was centrifuged and the supernatant was analyzed for the dye removal percentage using UV-spectroscopy at 664nm. The final concentration of MB at the equilibrium was measured from the calibration curve.

In order to compare the extent of MB uptake by the different activated carbon samples once the equilibrium was achieved (q_e; mg/g) was calculated by means of the following expression:

$$\text{percentage removal} = \frac{Co-Ce}{Co} * 100 \qquad 3.7$$

$$\text{Adsorption capacity} = \left(\frac{Co-Ce}{W}\right) * V \qquad 3.8$$

Where: C_0 (mg/L) is the initial concentration of MB and Ce is the concentration of MB at equilibrium. V (L) is the volume of MB solution in the flask and W (g) is the mass of activated carbon used in the experiment.

3.7.1 Calibration Curve Plot

Plotting standard curve was important for calculating the final concentration of MB from absorbance which is in return important for calculating percentage of color removal and adsorption capacity. For this reason different MB concentrations (0, 1, 2, 3, 4 and 5mg L^{-1}) were prepared and their respective absorbance were measured using UV-spectrophotometer. Finally linear relationship of absorbance versus concentration of MB were plotted and equation for final concentration of MB were found from the slope of the graph.

$$\text{Aabsorbance} = \text{slope} * Ce + y - \text{intercept} \qquad 3.9$$

3.7.2 Optimization of Adsorbent Dosage

Optimum value of adsorbent dosage for maximum removal of methylene blue dye were evaluated by means of conducting a batch adsorption study using AC sample with highest surface area(AC-151). 100 ml of MB solution with concentration of 10 mg L^{-1} were added in to five 250 ml conical flasks each containing different masses of AC sample (0.01, 0.03, 0.05, 0.07 and 0.1g). Then the mixture were allowed to be agitated in a shaker incubator at room temperature until equilibrium was reached. After filtration using wathmann filter paper Supernatant solution were taken in to a UV-spectrophotometer at a wavelength of 664 nm (wave length of maximum absorbance for MB) to determine the percentage absorbance of MB solution. Final dye concentration were found from

calibration curve so that percentage removal of dye and adsorption capacity, q_e (mg g^{-1}) were calculated using equation (3.7) and (3.8). Finally adsorbent dosage with maximum adsorption capacity can be considered as optimum value for adsorption experiment.

3.7.3 Optimization of Contact Time

In order to analyze the effect of contact time on the adsorption process, experiment were carried out by varying the duration (20, 40, 60, 80.100 and120 min). 0.05 g of AC sample were taken in to five different conical flasks (250 ml) and 100ml of prepared standard MB solution having PH of 10 were added to each conical flasks. Then the mixture were allowed to be agitated at room temperature for 60 min. At the end of the each time period samples were filtered and their respective absorbance were recorded from the UV-spectrophotometer reading. Finally percentage removal and adsorption capacity were calculated accordingly to select the best duration for maximum MB adsorption.

3.7.4 Optimization of PH

For determination of optimum PH value for maximum removal of the dye, the batch type adsorption experiments were carried out at various solution PH (range: 3-12) by adding the required volumes of 1M HCl or NaOH solution. 0.05 g of AC -151 was agitated with 100 ml standard solution of methylene blue dye in each conical flasks for 60min at room temperature. The pH of the dye solution was measured by using digital pen type PH meter. Adsorption experiments were carried out and the dye removal percentage was calculated using the relationship as mentioned earlier.

3.7.5 Optimization of Initial Concentration of Dye

To determine optimum initial concentration of MB, 100 ml of standard MB solution at a concentration of (10, 20, 30, 40 and 50 mg L^{-1}) were added in to a series of 250 ml conical flasks each containing 0.05g activated carbon. The mixture were then agitated at room temperature until equilibrium were achieved. At the end of the appropriate time supernatant were collected and percentage absorbance of each sample were recorded from the UV-spectroscopy reading. Finally percentage removal and adsorption capacity were determined from the relation mentioned above so that sample with highest adsorption capacity can be selected as the best condition for adsorption of MB.

3.8 Adsorption Kinetics

Kinetics study of the adsorption process is a fundamental procedure since it provides a relevant information about mechanism and characteristics of adsorption process follows which have a direct influence on the rate controlling step of the process. Pseudo-first order and pseudo-second order kinetics models are of the most commonly used kinetics models used to fit data obtained from the adsorption experiment. In this study kinetic experiments for MB uptake were carried out by adding 0.05 g of AC to a 100 mL of MB solution (10 mg L^{-1}) in a shaker at 25 °C for differing contact time (20,40,60, 80 ,100 and 120 min)

The residual concentration of MB, C (t), was measured as a function of time, and the uptake q (t) was calculated using the following equation:

$$q_t = \frac{C_o - C_t}{w} * V \qquad 3.10$$

Where: $C_{(t)}$ is the concentration of MB at time t (h). $q_{(t)}$ is the adsorption capacity at time t. V is the volume of MB solution used in ml. w is the grams of adsorbent used for the adsorption.

Finally the two proposed kinetic models were used to analyze the adsorption data so that one can suggest that which model best fit with the adsorption system.

3.8.1 Pseudo-First Order Model

First order kinetics model is developed based on solid adsorption capacity and Lagergren expresses it by rate expression as follows:

$$\frac{dq_t}{dt} = K_1(q_e - q_t) \qquad 3.11$$

Integrating and applying boundary conditions $q_{t|t=0} = 0$ and $q_{t|t} = t = q_t$ we get,

$$\log(q - qt) = \log qe - \frac{K1t}{2.303} \qquad 3.12$$

Where qt is the amount of MB on the surface of the activated carbon at time t (mg g^{-1}) and k_1 is the equilibrium rate constant of the pseudo-first-order adsorption (min-1).

Values of q_e and K_1 can be obtained from the slope and intercept of linear plot log ($q_e - q_t$) versus t indicating the applicability of Pseudo-first-order kinetic model (Gonawala & Mehta, 2014).

3.8.2 Pseudo-Second Order Model

Is expressed by the rate expression:

$$\frac{dq_t}{dt} = K_2(q_e - q_t)^2 \qquad 3.13$$

Integrating the above equation and applying boundary conditions $q_{t|t=0} = 0$ and $q_{t|t} = t = q_t$ gives:

$$\frac{1}{(q_e - q_t)} = \frac{1}{q_e} + K_2 t \qquad 3.14$$

It can be rearranged to linear form as:

$$\frac{t}{q_t} = \frac{1}{K_2 q_e^2} + \frac{t}{q_e} \qquad 3.15$$

Values of q_e and K_2 can be evaluated from linear plot of t/q_t versus t. Where: K_2 is the rate constant of the pseudo second order adsorption (g/mg.min) qt the amount of MB on the surface of the activated carbon at any time t (mg g^{-1}), q_e is the amount of dye adsorbed at equilibrium (mg g^{-1}) (Gonawala & Mehta, 2014).

3.9 Adsorption Isotherms

Adsorption equilibrium study is the most significant step while working with adsorption process. The data obtained from it are helpful in model prediction for analysis and design of an adsorption process. Several equilibrium isotherm equations have been used for representing experimental sorption isotherm as illustrated by different researchers. The most commonly used isotherm model equations are that of Langmuir's and Freundlich models. Accordingly the experimental sorption isotherm data which is obtained from batch experimentation is expected to be evaluated and best fitted into both the Langmuir and Freundlich isotherms models from which the experimenter is capable of selecting the best one among using the values the proposed model parameters. In this study Adsorption isotherm experiments were conducted by adding 0.05 g of AC to a 100 ml of different initial concentrations (10, 20, 30, 40 and 50 mg L^{-1}) of the dye to be adsorbed, and the adsorption process was carried out in a shaker at 25 °C for an optimum time. After the adsorption was finished, the adsorbent was filtered and the equilibrium concentrations were calculated by its respective equation. The two proposed isotherm models mentioned above were used to analyze the adsorption data using their respective model equation expressed below.

3.9.1 Langmuir Isotherm Model

Langmuir isotherm model was developed assuming that, (a) maximum absorption occurs when the adsorbent surface is covered by a single molecular layer of soluble material, (b) The absorption energy is fixed and identical at all the points, (c) The molecules of adsorbed material cannot move in the adsorbent surface. It is applicable for homogeneous surface adsorption (Gonawala & Mehta, 2014) and given by:

$$q_e = q_m \frac{K_L C_e}{1 + K_L C_e} \quad 3.16$$

Where q_e and q_m (mg g^{-1}) are the adsorbed amount at equilibrium and Langmuir maximum adsorption, respectively; K (mg L^{-1}) is the constants of Langmuir.

Above equation can be rearranged in to linear form as:

$$\frac{C_e}{q_e} = \frac{1}{q_m K_L} + \frac{C_e}{q_m} \quad 3.17$$

Langmuir constants can be obtained from the plot of C_e versus C_e/q_e.

The essential characteristics of Langmuir isotherm is expressed by a separation or equilibrium parameter, which is a dimensionless constant defined as:

$$R_L = \frac{1}{K_L C_o} \quad 3.18$$

Where; R_L indicates the nature of adsorption as: Unfavorable R_L>1; Linear R_L =1; Favorable 0 < R_L<1; Irreversible R_L =0 (Gonawala & Mehta, 2014).

3.9.2 Freundlich Isotherm Model

One of the most popular adsorption isotherms used for liquids to describe adsorption on a surface having heterogeneous energy distribution is Freundlich isotherm (Gonawala & Mehta, 2014). Freundlich isotherm is derived assuming heterogeneity surface and presented in a logarithmic scale using the expression:

$$q_e = K_F Ce^{1/n} \quad 3.19$$

Where: q_e =the Equilibrium loading in mg/ g, C_e is the Equilibrium concentration in mg/L, K_F is adsorption capacity in mg/g and n is the adsorption intensity.

Above equation can be rearranged in to linear form as:

$$\log q_e = \log K_F + \frac{1}{n}\log C_e \quad 3.20$$

A plot of log q_e versus log C_e gives a straight line, with a slope of 1/n and intercept of log K_F. The value of Freundlich constant (n) should lie in the range of 1–10 for favorable adsorption, higher n value the better the adsorption (Gonawala & Mehta, 2014).

3.9.3 Temkin isotherm model

Temkin isotherm based on the ions sorption heat, which is due to the sorbate and adsorbent interactions, is given by the following equation:

$$q_e = \beta \ln k_T + \beta \ln C_e \quad 3.21$$

Where, K_T is the equilibrium binding constant (L mol^{-1}) corresponding to the maximum binding energy and constant the value of constant B is related to the heat of adsorption and is given by:

$$\beta = \frac{RT}{b}$$

Where b is Tempkin isotherm constant of binding energy (J/mol K). The negative sign of B values for adsorbents shows that adsorption is exothermic. Both Kt and B can be determined from a plot qe versus ln Ce

4 RESULT AND DISCUSSION

4.1 Proximate and Elemental Analysis of FWB

Table 4.1 Results of proximate analysis for flower, stem and leaf

Components	Flower	Stem	Leaf
Moisture content (wt %)	8.07	9.16	11.60
Volatile matter content (wt %)	70.14	68.12	62.90
Ash content (wt %)	5.66	7.45	13.23
Fixed carbon content (wt %)	16.13	15.27	12.27

Table 4.2 Results of elemental analysis of FWB precursor

Element	Percentage (wt %)
Carbon	49.57
Hydrogen	6.25
Nitrogen	2.98
Sulfur	0.07
Oxygen	41.13

Table 4.1 shows the results of Proximate analysis of FWB in which FWB contains 9.61 % moisture content, 67.05% volatile matter content, 8.78% ash content and fixed carbon content of 14.56%. From the result it can be seen that FWB had lower ash content and higher volatile matter content which makes it a good starting material for AC production. It is also discussed by (Kumar & Jena, 2015) as higher volatile matter content and low ash content of a biomass resource makes it a good raw material for preparing activated carbon. The low ash content would result in minimal effects of inorganic impurities on pore development \during activation process. Ultimate analysis results in (Table 4.2) indicates that FWB is contained of 49.57% of carbon, 6.25% of hydrogen, and 2.98% of nitrogen. 0.07% sulfur and 41.13% oxygen. From this it can be seen that FWB is mainly composed of carbon, oxygen and hydrogen which is expected in most cellulosic materials and can be used as a raw material for the preparation of activated carbon due to its high content of carbon.

Flower part of the biomass contains a relatively higher value of fixed carbon and volatile matter content as compared to stem and leaf. Regarding the ash content flower part had smaller value than the stem and the leaf parts. For this study equal mass of flower and stem part of the biomass were used as a raw material for the preparation of activated carbon since the leaf part contains lower fixed carbon content and higher ash content.

Table 4.3 BBD experimental design matrix and results of corresponding response variables

S.N	I.R $ZnCl_2$:FWB	Temp. (^0C)	Time (hr)	Yield (%)	Iodine.N (mg g^{-1})	BET S.area (m^2 g^{-1})
1	0.5:1		1	47.56	408.27	419
2	1:1		1.5	45.42	431.5	444
3	1:1	400	0.5	46.08	455.38	469
4	1.5:1		1	43.82	506.9	517.37
5	0.5:1		1.5	33.88	463.11	475
6	0.5:1		0.5	39.72	447.83	464
7	1:1		1	37.4	_	_
8	1:1		1	36.92	_	_
9	1:1		1	37.1	714.0	_
10	1:1		1	36.87	_	_
11	1:1	500	1	37.03	718.33	750
12	1.5:1		0.5	34.84	522.13	542.89
13	1.5:1		1.5	24.98	587.05	604
14	0.5:1		1	22.08	513.89	522.6
15	1.5:1		1	19.66	451.62	488
16	1:1		1.5	17.52	542.10	560.05
17	1:1	600	0.5	21.04	449.73	467

4.2 Statistical Analysis of the Experimental Results

In this study RSM based on BBD was used to investigate the effect of impregnation ratio, activation temperature and activation time on the preparation of AC using Design-expert software 7.0.0. The statistical significance of the model was analyzed using ANOVA as shown in Table 4.4.

Table 4.4: Analysis of variance for Response Surface Quadratic Model of AC from FWB

Source	Sum of Squares	df	Mean Square	F Value	p-value Prob > F	
Model	2.48E+05	9	27504.62	112.8	< 0.0001	Significant
A-impregnation ratio	7716.55	1	7716.55	31.65	0.0008	
B-temperature	4659.99	1	4659.99	19.11	0.0033	
C-time	2526.18	1	2526.18	10.36	0.0147	
AB	4106.89	1	4106.89	16.84	0.0046	
AC	578.64	1	578.64	2.37	0.1673	
BC	3483.95	1	3483.95	14.29	0.0069	
A^2	50299.86	1	50299.86	206.28	< 0.0001	
B^2	98253.62	1	98253.62	402.94	< 0.0001	
C^2	53032.81	1	53032.81	217.49	< 0.0001	
Residual	1706.91	7	243.84			
Lack of Fit	1706.91	3	568.97	1.42		Insignificant
Pure Error	0	4	0			
Core Total	249248.5	16				

The Model F-value of 112.80 implies the model is significant. There is only a 0.01% chance that a "Model F-Value" this large could occur due to noise. Values of "Prob > F" less than 0.0500 indicate model terms are significant. The lack of Fit F-value of 1.42 implies the Lack of Fit is not significant relative to the pure error. Non-significant lack of fit is good and shows that the above model is appropriate to predict the BET surface area of the activated carbons within the range of variables studied.

In this case A, B, C, AB, BC, A^2, B^2, C^2 are significant model terms. Values greater than 0.1000 indicate the model terms are not significant.

Table 4.5: R-squared (R^2) value for the model

Std. Dev.	15.62	R-Squared	0.9932
Mean	573.87	Adj R-Squared	0.9843
C.V. %	2.72	Pred R-Squared	0.8904
PRESS	27310.53	Adeq Precision	29.165

The "Pred R-Squared" of 0.8904 is in reasonable agreement with the "Adj R-Squared" of 0.9843."Adeq Precision" measures the signal to noise ratio. A ratio greater than 4 is desirable. Your ratio of 29.165 indicates an adequate signal.

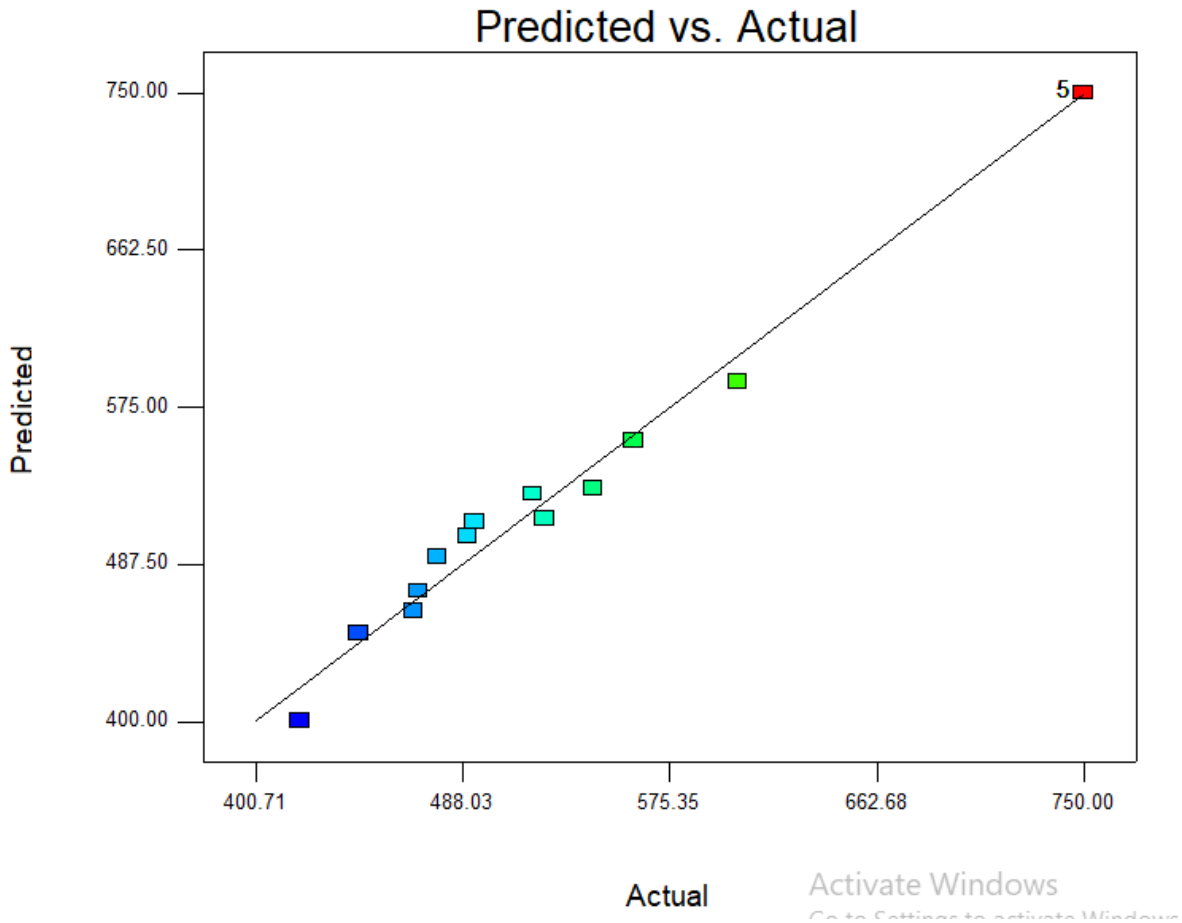

Figure 4.1: Diagnostic plot for the fitted model

The actual and predictive model in terms of coded and actual factors is presented below. This terms can be used to regenerate the results of this experiment, but they can not be used for modeling future response.

Final Equation in Terms of Coded Factors:

AC surface area = +750.00 +31.06 * A + 24.14 * B +17.77 * C - 32.04 *A* B + 29.51* B * C - 109.30* A^2 -152.76* B^2 -112.23* C^2 4.1

Final equation interms of actual factors:

AC surface area= -4198.70875 + 1256.93000 * impregnation ratio + 15.56783 *temperature + 10.63742 * time - 0.64085 * impregnation ratio * temperature + 9.83750E-003 * temperature * time - 437.19500* impregnation ratio^2 - 0.015276* temperature^2 -0.12470 *time^2 4.2

4.3 Effect of Activation Process Variables on Response Variables

4.3.1 Main Effect on Response Variables

4.3.1.1 Effect of Impregnation Ratio on Yield of Activated Carbon

The effect of impregnation ratio on AC yield was studied by varying its value from 0.5, 1 and 1.5 at different temperature values (400, 500 and 600 ^oC). Production yield of activated carbon was calculated by dividing mass of biomass after carbonization to mass before carbonization. The result presented in fig: 4.2 showed that yield decreases continuously from 39.72% to 24.98% as impregnation ratio increases from 0.5 to 1.5 at 400 ^oC. That is due to the continuous degradation of biomass components at increased temperature. Carbonization of FWB without impregnation by $ZnCl_2$ at 500 ^oC results higher AC yield of 67.14%. This is due to the reason that activation without activating agent end up with minimum degradation of biomass components and little evolution of volatile matters.

Table 4.6 AC yield at different impregnation ratio

IR	Yield(%)-500^{o}C	yield(%)-400^{o}C	Yield(%)-600^{o}C
0.5	39.72	47.56	22.08
1	36.87	45.42	21.04
1.5	34.84	43.82	19.66

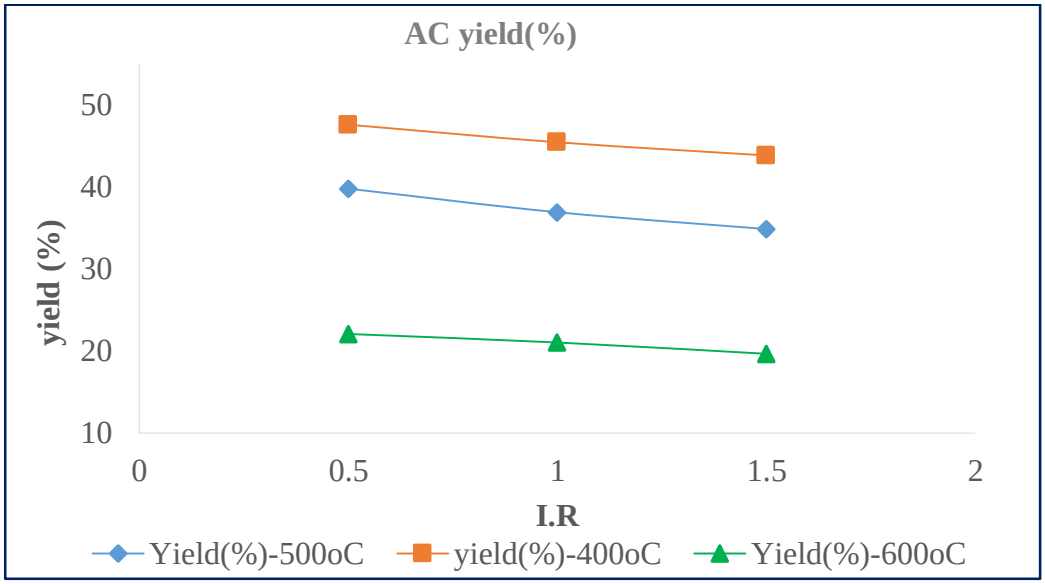

Figure 4.2: Effect of impregnation ratio on AC yield

4.3.1.2 Effect of Impregnation Ratio on BET Surface area

With the change in impregnation ratio there was a difference observed in BET surface area of AC. Surface area of the produced AC were increased from 475 to 750 $m^2 g^{-1}$ as impregnation ration increases from 0.5 to 1. However, when impregnation ratio further increased from 1 to 1.5 (Fig. 4.3) surface area were decreased to 604 $m^2 g^{-1}$. This might be because of at higher impregnation ratio pores produced will become widened and some are collapsed. Considering the difference in BET surface area, the impregnation ratio of 1:1 was chosen to produce AC from FWB.

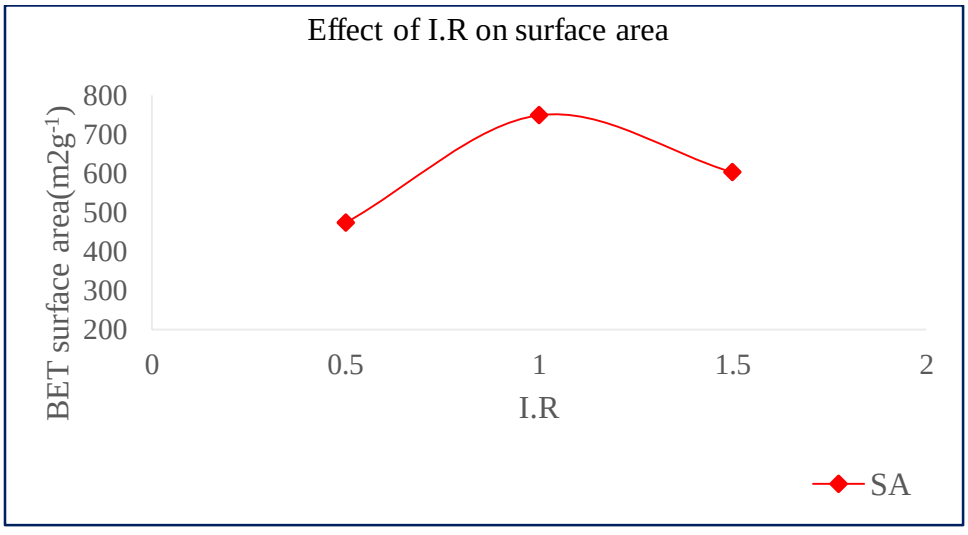

Figure 4.3: Effect of impregnation ratio on AC surface area

4.3.1.3 Effect of Temperature on AC Yield

The effect of different activation temperature (400, 500 and 600 ºC) on AC yield were illustrated in (fig: 4.4). From the figure it can be understood that AC yield decreases from 47.56 at 400ºC to 22.08 at 600ºC. The successive decrement of AC yield with increasing in activation temperature is because of higher degradation of biomass at higher temperature which results in loss of weight.

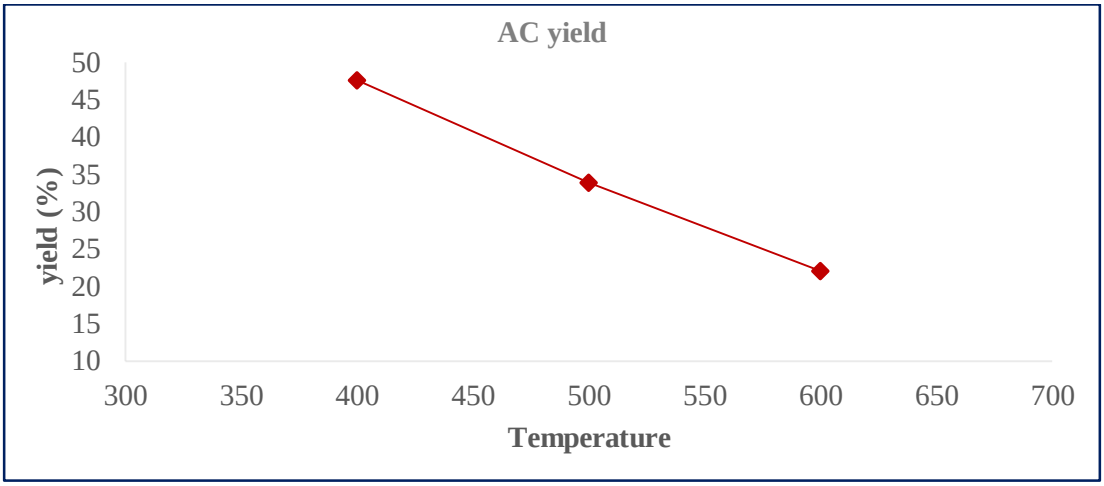

Figure 4.4: Effect of activation temperature on AC yield

4.3.1.4 Effects of Temperature on BET Surface area

The effect of activation temperature on AC surface area were investigated in the range of 400 to 600 ^{O}C and the results are presented in (Fig: 4.5). As indicated in the figure it was observed that surface area increases with increase in activation temperature from 400 to 500 ^{O}C but decreases with further increase in activation temperature to 600 ºC. Surface area increases from 517.3m^2 g^{-1} to 750 m^2 g^{-1} when the activation temperature is changed 400 ^{O}C to 500 ^{O}C. Evolution of volatile matter contents due to heat effect were intense up to 500 ^{O}C as a result it creates pores. Hence, surface area increases. Surface area decreases from 750 m^2 g^{-1} to 560.05 m^2 g^{-1} while temperature is changed from 500 ^{O}C to 600 ^{O}C. The decrease in surface area above 500 ºC was e to the shrinkage and closing up of produced pores at higher temperature. Consequently activation temperature of 500 ºC were selected as an optimum operating condition for AC preparation from FWB in this experiment. At this temperature surface area of 750 m^2 g^{-1} were obtained. Similar trends have

reported by (Bedmohata MA, Chaudhari AR, Singh SP, & Choudhary, 2015) who studied preparation of activated carbon from lignin using H_3PO_4 for methylene blue removal.

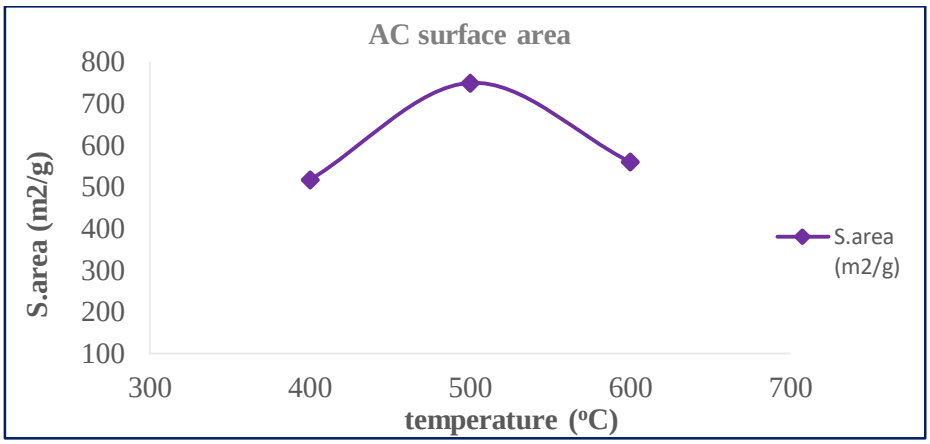

Figure 4.5: Effect of variation of activation temperature on AC surface area

4.3.1.5 Effects of Temperature on Iodine Number

It has been observed from the experimentation that the iodine number increase from 533 mg g^{-1} to 803.11 mg g^{-1} as the activation temperature raised from 400 °C to 500 °C but the iodine number gets decreased from 803.11 mg g^{-1} to 583.14 mg g^{-1} as the temperature increase to 600 °C (see Fig:4.6). From this we can understand that ZnCl2 activation of FWB were effective at a temperature of 500 °C. During the initial stage of activation salt attack resulted in an extensive evolution of CO, CO_2 and methane were occurred (which could not occur under simple heat treatment without activating agent like $ZnCl_2$). As the temperature reaches to 500 °C the weight of biomass decreases significantly and the biomass structure becomes dilate which results in the development of pores. However further increment on temperature to 600 °C results a decreasing effect on the iodine number of the AC. This might be due to collapsing or shrinkage of char. Similar effect of temperature has been reported by (On, n.d.) who studied Production and characterization of Activated Carbon produced from a suitable Industrial sludge. The experimental factors affected iodine number in similar way as they did on surface area. Thus, the effect of other variables on iodine number is not discussed to remove redundancy.

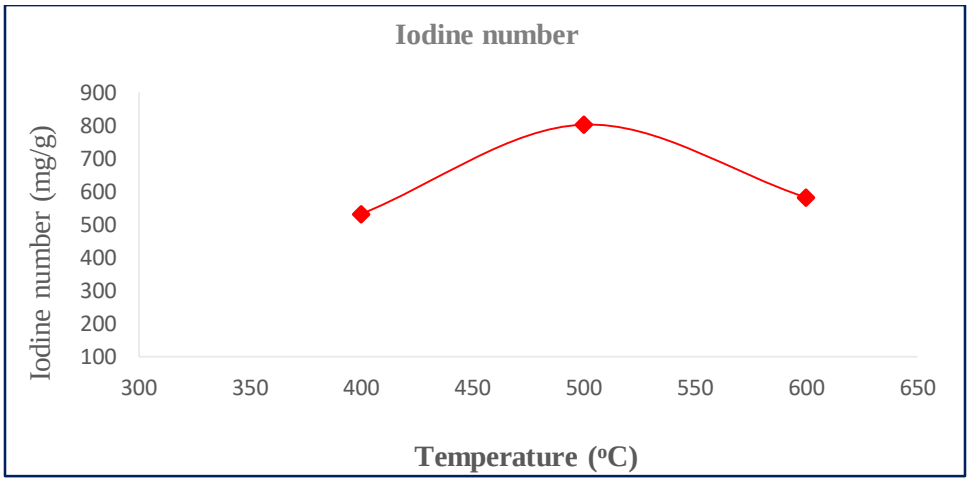

Figure 4.6: Variation of AC iodine number with different activation temperature

4.3.1.6 Effects of Activation Time on AC Yield

Under this experimentation variation of time under the range of 0.5 to 1.5 hr at 500 °C activation temperature resulted in different AC yield value as shown in (Fig: 4.7). As it is presented in the figure AC yield decreases from 39.72 to 24.98 % with increasing the activation time from 30min to 90 min. This attributed to the release of volatile matters along with the formation of pores and prolonged carbonization time may resulted in pore collapse and an increased proportion of meso and macropores. Similar variation of AC yield were also observed for other temperatures. The result is also in line with literature. (Ozdemir et al., 2014) studied Preparation and characterization of activated carbon from grape stalk by zinc chloride activation and reported similar effect of activation time. Under this study Preparation of AC activation period of 1hr was chosen to get AC with required and desired properties.

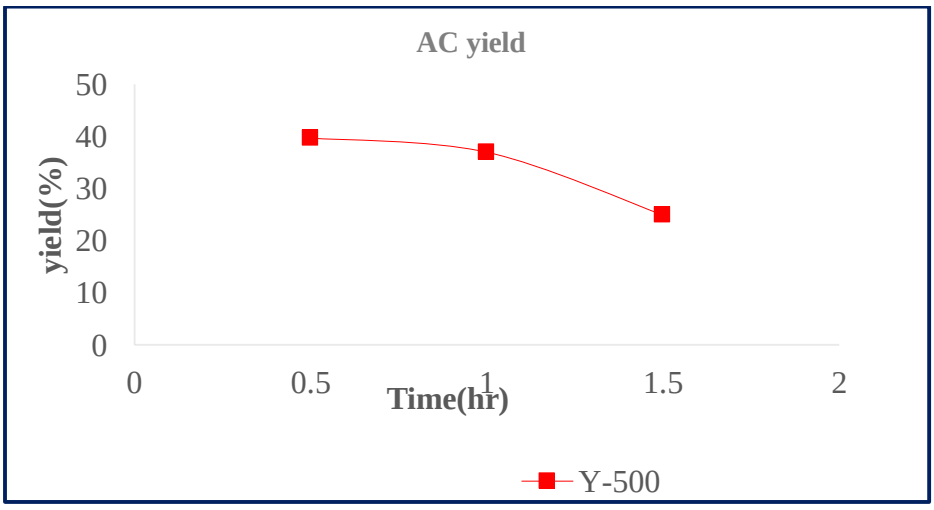

Figure 4.7 The effect of activation time on AC yield

4.3.1.7 Effects of Time on BET Surface Area

AC samples produced at different activation period were analyzed for their respective surface area and it was noted that it was strongly affected by time of activation. As time increases from 30min to 60min at activation temperature of 500 ^{o}C BET surface area of AC produced from FWB were increased from 542.89 $m^2 g^{-1}$ to 750 $m^2 g^{-1}$. Thereafter, BET surface area gradually decreased to a value of 604 $m^2 g^{-1}$at 90 min of activation time (see Fig: 4.8). Thus, activation period of 60 minute can be considered as a good operating time in this study. The decrease in BET surface area of AC for the activation time period of 60 min to 90 min is considered to be due to the extended activation of the product, resulting in shrinkage of char structure and widening and combining of some micro pores into mesopores.

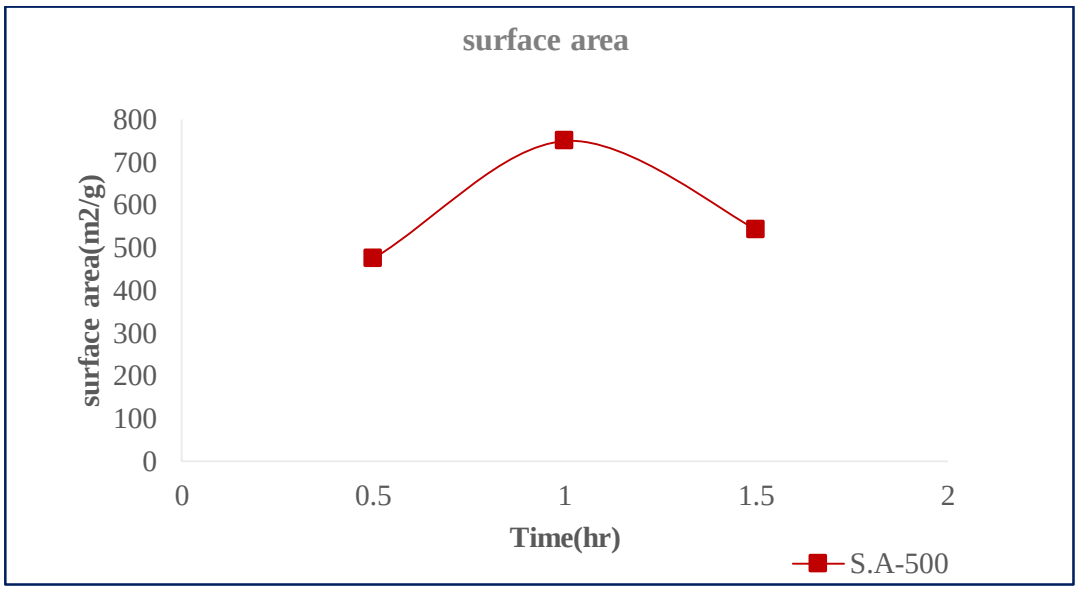

Figure 4.8 Effect of activation time on AC surface area

4.3.2 Interaction Effect of Activation Process Variables on AC Surface Area

4.3.2.1 Interaction Effect of Impregnation Ratio and Activation Temperature

The combined effect of impregnation ratio and activation temperature on AC BET surface area at constant impregnation ratio (1:1) were presented using 3D response surface plot as shown in (Fig.4.9). As it can be seen from the figure, the two factors had a positive interaction on the surface area. Maximum BET surface area of AC is found in the red region which indicates that maximum surface area can be obtained at moderate activation temperature and moderate impregnation ratio. At activation temperature of 500 ^{o}C and impregnation ratio of (1:1), BET surface area of 750 m^2 g^{-1} were obtained.

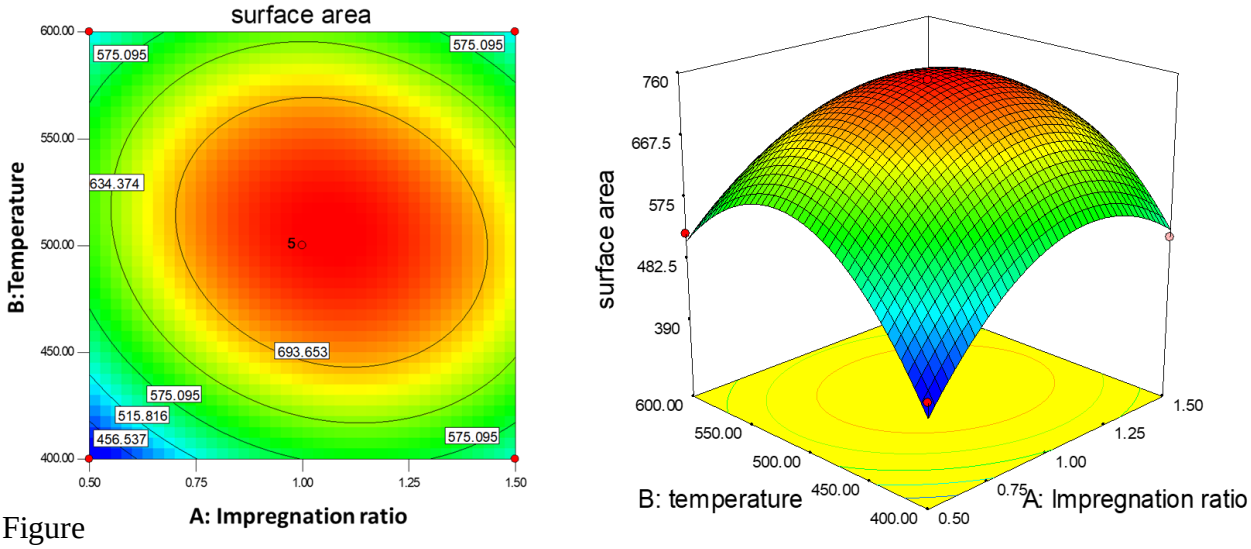

Figure 4.9: Contour and 3D surface plot for interaction effect of impregnation ratio and temperature on AC surface area

4.3.2.2 Interaction Effect of Activation Temperature and Time

Contour and 3D response surface plot shown in (Fig: 4.10) shows the interaction effect of activation time and activation temperature at constant impregnation ratio (1:1). At lower time and activation temperature surface area of AC experienced a minimum value while it had maximum value at medium activation temperature and activation time as shown in the dome shaped region of the 3D plot. At higher value of both factors the surface area resulted in decreased amount.

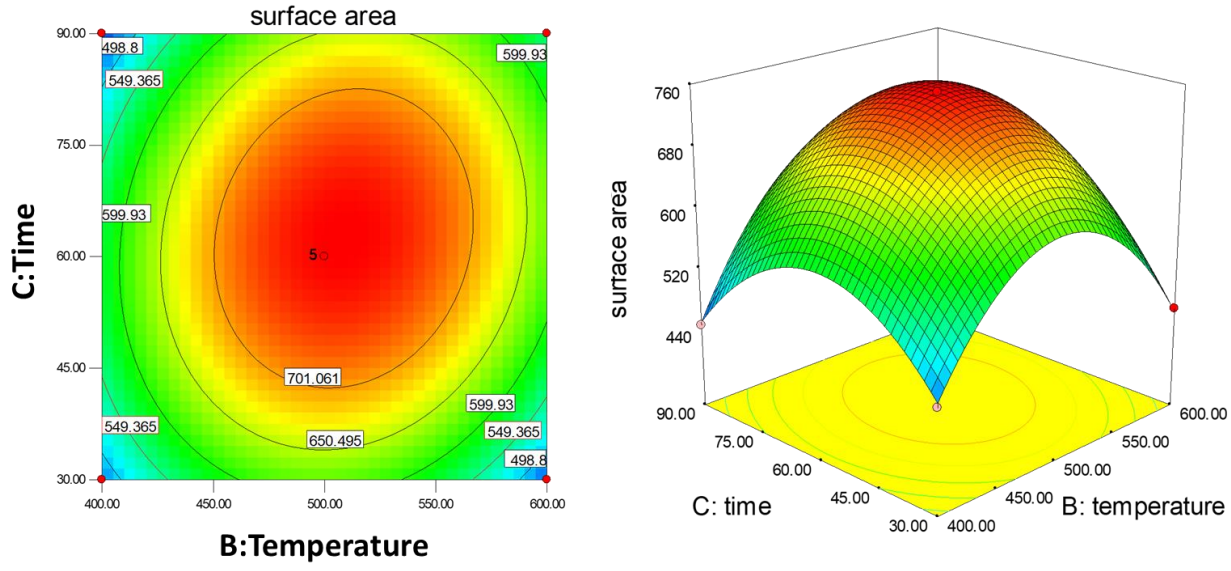

Figure 4.10: Contour and 3D surface plot for interaction effect of temperature and time on AC surface area

4.4 Characterization of FWB Based AC

4.4.1 Proximate Analysis of AC-151

Proximate analysis of activated carbon prepared from flower waste biomass were obtained experimentally through standard methods mentioned in the methodology part of the study (see Table: 4.7). As shown in the table results of proximate analysis shows the difference in fixed carbon content, moisture content, volatile matter content and ash content of the raw material as well as the produced activated carbon. AC derived from FWB contains high amount of fixed carbon content as compared with the raw material which shows a significant effect of the $ZnCl_2$ activation which increases the fixed carbon content from 14.55 % to 69.17 %. On the other hand volatile matter content of the raw material were 67.05 % and due to the activation it was decreased to a value of 14.38 %. This is due to vaporization of volatile components of the FWB during carbonization step at different temperature. Moisture content of the produced activated carbon also experience a decrease from 9.61 % to 6.14% due to the removal of some portion of moisture during activation. However ash content of activated carbon increases from 8.78 % to 10.31 %. This might be due to the formation of inorganic residue during activation.

Table 4.7: proximate analysis of activated carbon from FWB

		Moisture content	Ash content	Volatile matter content	Fixed carbon content
FWB		9.61	8.78	67.05	14.55
FWB + $ZnCl_2$ (AC-151)	500°C	6.14	10.31	14.38	69.17

4.4.2 Surface Area and pore development

The N_2 adsorption desorption isotherm for AC produced from FWB at different temperature and impregnation ratio has been presented in (Fig 4.11 A and B) by plotting relative pressure versus volume of gas adsorbed at STP. The shape of the isotherm can provide a qualitative information about the porosity of the prepared activated carbon. According to the IUPAC classification, the N_2 adsorption desorption isotherms of the AC samples are a combination of type I (at low relative pressures) and type IV (at moderate and high pressures). A rapid rise in the isotherm is observed at low relative pressure which indicates the production of more micropores, followed by horizontal plateau at moderate and higher relative pressures with knee which corresponds to the development of larger micropores and mesopores. The continuous N_2 uptake at very high relative pressure near 1.0 indicates the presence of macropores (Kumar & Jena, 2015).

As it can be seen from the Fig. 4.11A, increasing the activation temperatures from 400 to 500°C lead to the development of micropores, as revealed by the rapid rise in adsorbed N_2 amounts at low relative pressures. However, the N_2 uptake at moderate and high relative pressure increased gradually, indicating the formation of mesoporosity and some macroporosity. On the other hand, at higher temperatures of 600 °C the isotherm forms narrow knee structure with decreases in N_2 adsorption at low relative pressures which is indicative of widening of the microporosity and gradual increase of mesoporosity.

Similarly, from Fig. 4.11B, N_2 uptake increases sharply at low relative pressures as the impregnation ratio increases from 0.5 to 1, revealing the formation of micropores and then isotherms gradually becomes narrow knee and N_2 adsorption increased slowly at moderate and high relative pressures as the impregnation ratio increases from 1 to 1.5 which results in progressive widening of the existing microporous structure and a slight increase of mesoporosity.

.

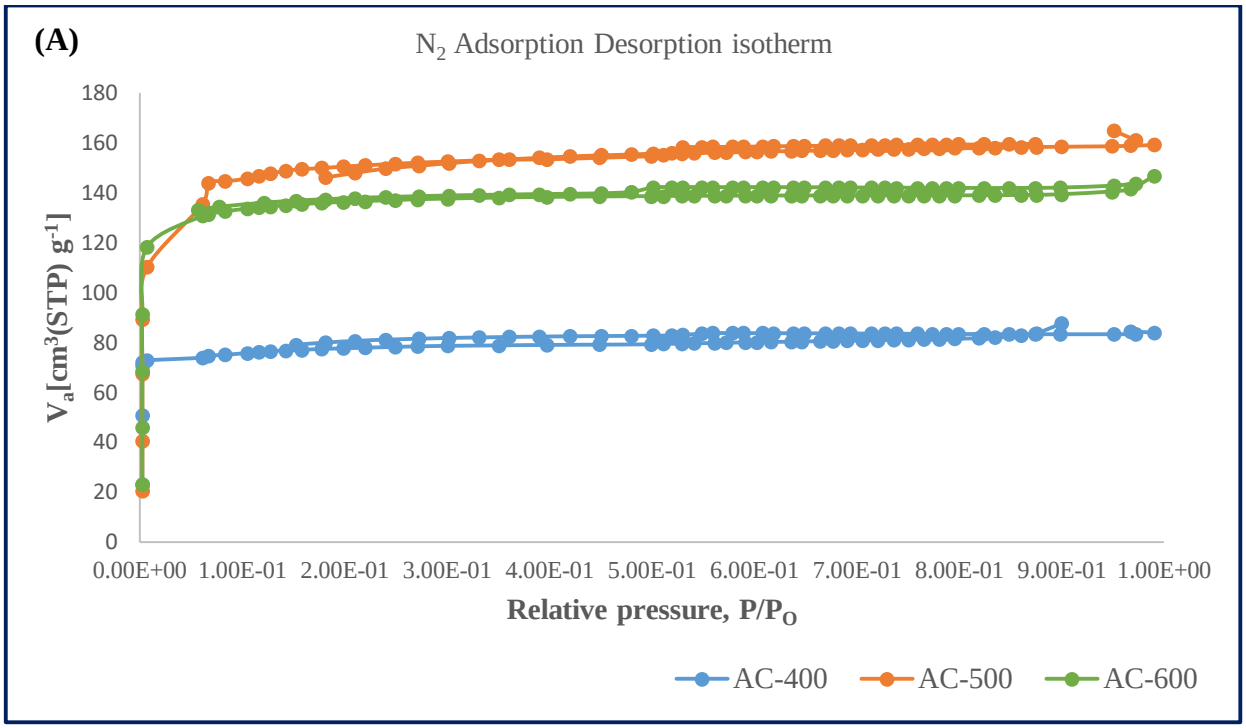

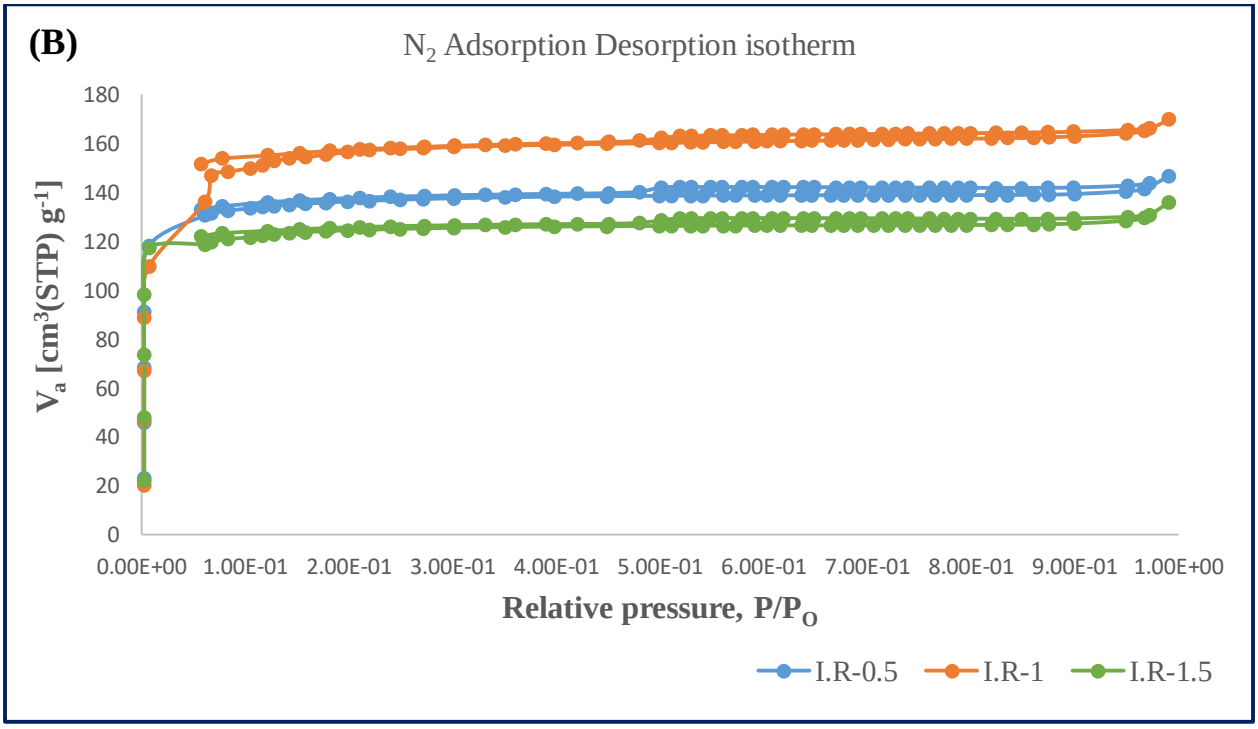

Figure 4.11: N_2 Adsorption Desorption isotherm of AC, (A) at different activation temperature, (B) at different impregnation ratio

The pore size distributions of the prepared AC at different activation temperatures and impregnation ratios are shown in Fig. 4.12 A and B. Adsorbent pores are classified into three groups: micropore (diameter < 2 nm), meso-pore (2–50 nm), and macropore (>50 nm) (Sayğılı & Güzel, 2018). As it can be seen from the figures the pore diameter of the AC ranged from 0.2 nm to 43 nm for all temperatures. This attributed to the formation of micro and meso pore AC. However, most of the pore diameters lie between 0.2 -2 nm indicating that the AC pore diameters are in the micropore range. From this figure, it can be seen that lower (400) and higher temperatures (600 ^{o}C) and impregnation ratios resulted in wider pore size and lower BET surface area. Similarly, at lower impregnation ratio pore size is larger because the activating agent is insufficient to attack the whole biomass structure. But, at medium impregnation ratio and activation temperature maximum pore formation was achieved as a result BET surface area increased. At higher ratio pore widening and shrinkage due to excessive chemical attack increased the pore diameter which results in decreased surface area.

The pore size distribution of samples in this study are more of micro porous. Table 4.8 summarizes the surface area and pore volume of the ACs.The produced activated carbon had a surface area of 750 $m^2 g^{-1}$ total pore volume of 1.91 $cm^3 g^{-1}$ and pore diameter of 1.89 nm. While, stem part of the biomass had a surface area of 10.2 $m^2 g^{-1}$, total pore volume of 0.2589 $cm^3 g^{-1}$ and pore diameter of 101.52 nm. On the other hand the flower part of the biomass have 0.43 $m^2 g^{-1}$surface area, 0.005 $cm^3 g^{-1}$ total pore volume and 46.48 nm pore diameter. As compared to the raw materials AC have much larger surface area and minimum pore diameter. This is due to the effect of activation. Before activation the raw biomass is filled with more volatile matter contents and other degradable components which results in minimum pores but large pore diameter. However after activation the volatile components are removed so that pore increases reducing the pore diameter. In general activation of flower waste biomass increases the surface area from 0.43 $m^2 g^{-1}$to 750 $m^2 g^{-1}$ and reduces the pore diameter from 101.52 nm to 1.89 nm.

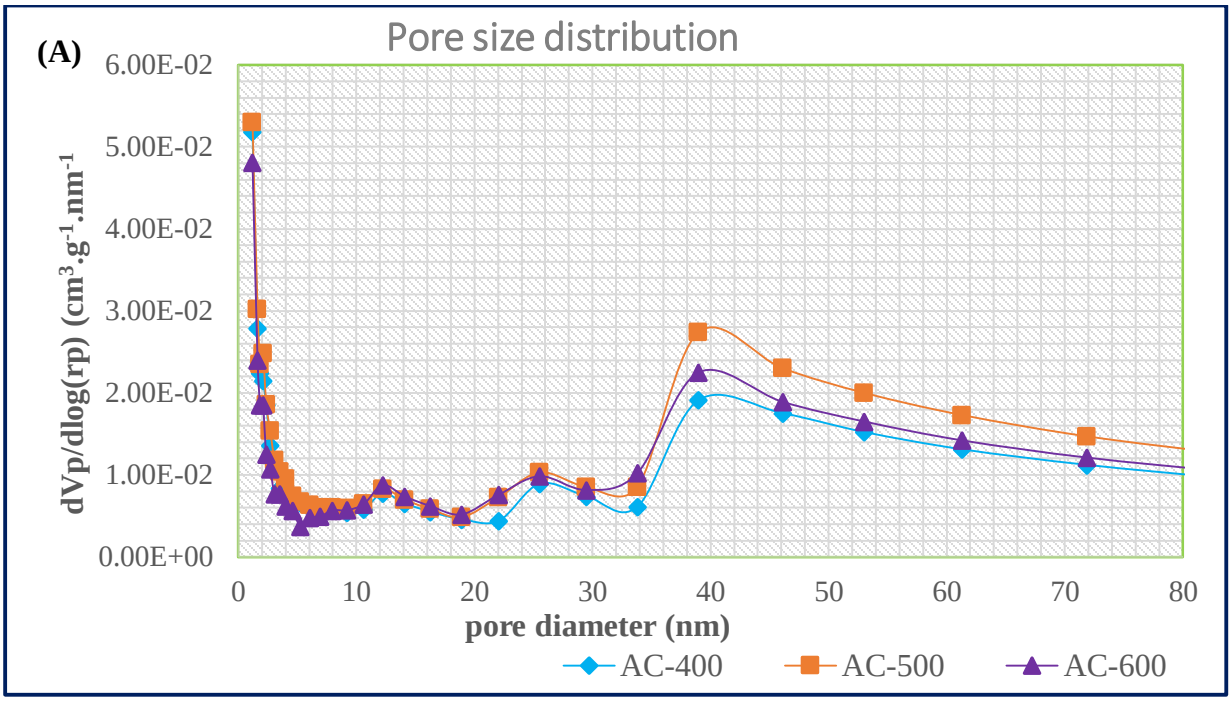

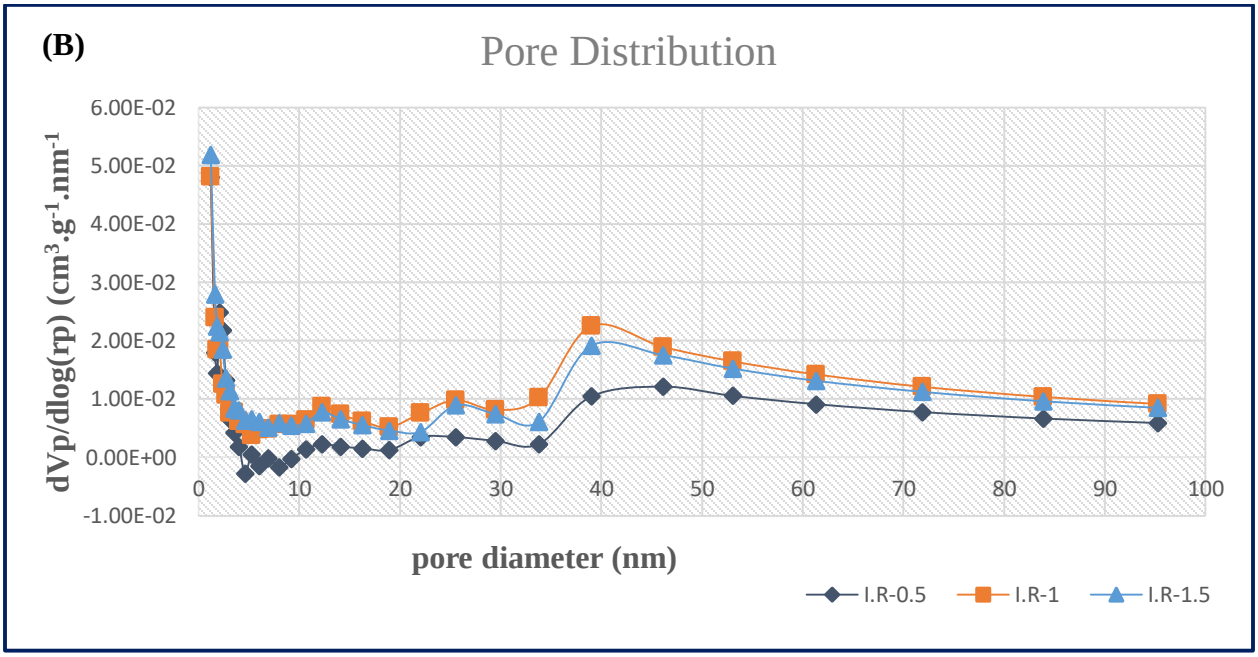

Figure 4.12: Pore size distribution of AC, (A) at different temperature, (B) different impregnation ratio

Table 4.8: Surface area and pore volume of raw material (stem &flower) and activated carbon (AC-151)

Sample	Activation condition	BET surface area(m^2g^{-1})	Pore volume (cm^3g^{-1})	Pore diameter (nm)
Flower		10.2	0.2589	101.52
Stem		0.43	0.005	46.48
AC-151	500ºC	750.0	1.91	1.89

4.4.3 SEM and EDS Analysis

The morphology of FWB derived AC was observed from the analysis of SEM micrographs (Fig: 4.14 A and B). Fig. 4.14A shows SEM image of AC at 550 magnification and it was found that the surface were irregular and rough surface. The same region observed using high (5000) magnification showed rough surface morphology with slit crack structures formed and fragmented heterogenic pore structures on the surface. These slits supported the existence of the low porosity indicated by analysis of the N_2 adsorption/desorption isotherms and facilitate the transfer of pollutants into the interior of the AC, thereby increasing the adsorption capacity of AC. The differences in the morphological structures attributed to the dehydrating effect of $ZnCl_2$, it removes oxygen and hydrogen from lignocellulosic material which promotes the development of porous structure.

In order to compare elemental composition of AC at different layers in the AC structure, EDS analysis were investigated on a small region at different accelerating voltage (3.705, 6.350 and 8.040 keV), thereby electrons of varying energy are generated which penetrated to different depths of the sample. The elemental analysis using the EDS study on AC sample suggested that the presence of different elements and carbon elements which signifies that the AC structure were mostly contained by carbon atom (87.97 %). The EDS analyses confirmed that almost homogenous distribution of elements under the investigated AC region (Fig: 4.14 C & D). As it can be observed from the spectra, the analysis confirmed the presence of carbon, and trace amounts of nitrogen, oxygen, sulfur, chlorine and zinc. Chlorine and zinc are in small atomic percentage which were remained inside the AC structure during washing. As compared to the carbon content of FWB

(49.57%) AC have increased carbon content (87.97%) which is resulted from activation using $ZnCl_2$.

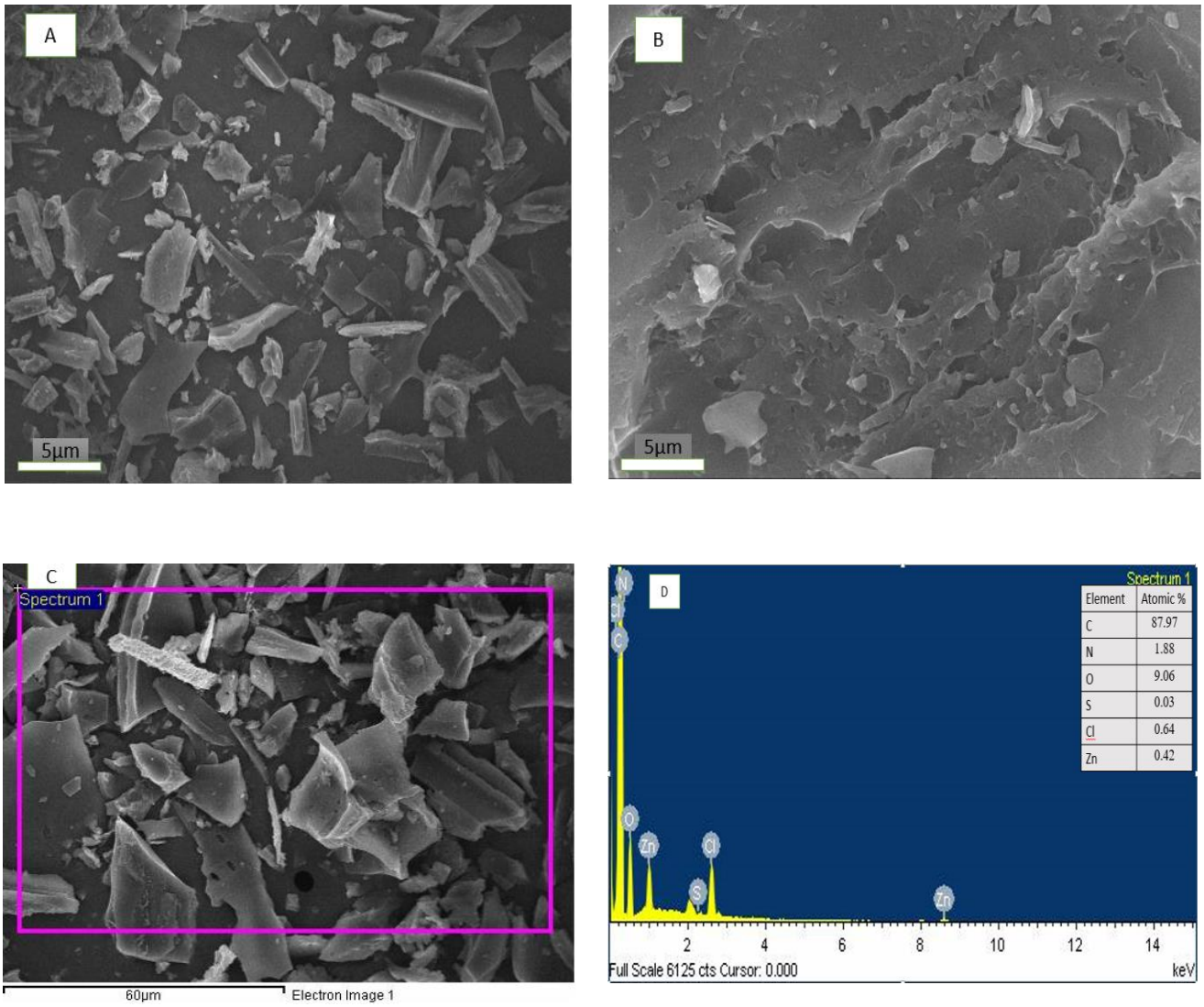

Figure 4.13: (A) SEM micrograph of AC at 550 magnification, (B) SEM micrograph at 5000magnification, (C) region of sample covered by the spectrum, and (D) EDS spectrum and atomic % of elements of AC produced from FWB at 500ºC, 1:1 and 1hr

4.5 Adsorption Experiment Analysis

4.5.1 Calibration Curve plot for MB Adsorption

The calibration curve plot for MB at a wave length of 664nm were obtained from the adsorption experimentation of MB using flower waste biomass derived activated carbon. It is important to determine the value of final concentration knowing the absorbance directly from the UV-spectroscopy. The result was presented as follows:

Table 4.9: Variation of absorbance with MB concentration

Initial MB concentration in (mg/l)	Absorbance (%)
0	0
2	194
4	0.387
6	0.597
8	0.843
10	1.085

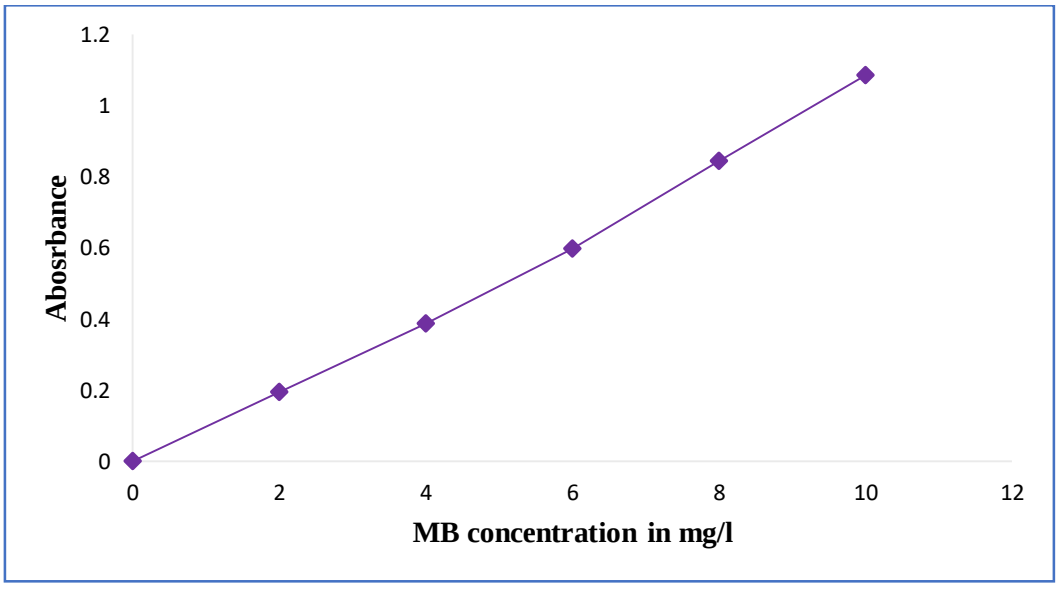

Figure 4.14: Calibration curve for methylene blue solution

From the graph the slope was found to be 0.108 so that final equilibrium concentration at any time can be determined by dividing absorbance to that of slope. C_e= absorbance/0.108.

4.5.2 Effects of Adsorption Experiment parameters

4.5.2.1 Effect of Adsorbent Dosage

The percentage removal capacity of activated carbon is due to their porous structure and pore size distribution, and it depends on the polarity, solubility and molecular size of adsorb ate (Bedmohata MA et al., 2015) The effect of adsorbent dosage on MB removal percentage is illustrated in fig 4.13 below. From the figure it is observed that percentage removal increases linearly with increasing amount in the adsorbent dosage up to 0.05 g. This is because of the increased amount of adsorbent active sites. But above 0.05 g a slight increment is observed on the percentage removal of MB. Even if percentage removal slightly increase beyond 0.05 g it might lead to increased cost of the adsorbent, as a result is preferred to take 0.05 g/100ml as an optimum adsorbent dosage for MB adsorption. At this adsorbent dosage (0.05 g/100ml) the percentage removal of MB were 93.62%.

Table 4.10**:** Effect of adsorbent dosage on MB removal

Dosage (g)	Absorbance	Ce (mg/l)	Percentage of removal
0.01	0.309	2.86	71.4
0.03	0.184	1.7	83.0
0.05	0.08	0.73	92.7
0.07	0.074	0.69	93.1
0.1	0.069	0.64	93.62

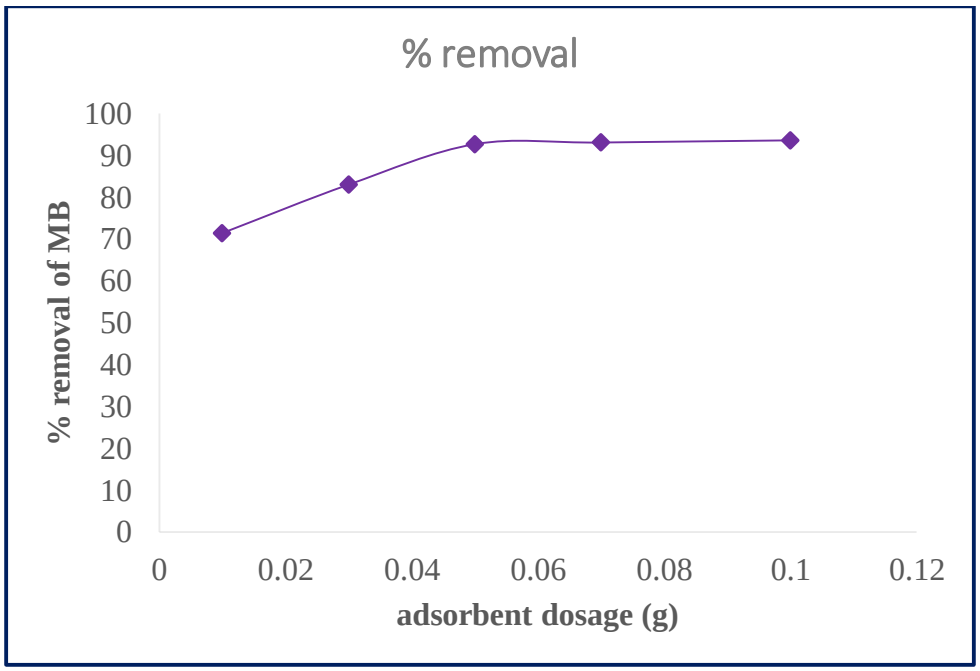

Figure 4.15**:** Effect of adsorbent dosage on percentage removal of MB at 10mg/l, PH 10 and contact time of 60min

4.5.2.2 Effect of PH

The effect of initial PH of MB solution on percentage removal were investigated by varying PH from 3 to 12 under constant adsorption parameters as mentioned in the methodology part. The results obtained from the experimentation are shown in (fig 4.17) below. From the figure it can be observed that removal percentage increases as PH value getting larger.it is evident that the removal percentage of MB increases from 84.2% to 92% as PH varies from 3 to 12. This is due to the reason that the surface of activated carbon is generally considered to be negatively charged, so that minimum value of MB removal percentage in the lower pH region would be expected as the acidic medium would lead to an increase in hydrogen ion concentration which would then neutralize the negatively charged carbon surface thereby decreasing the adsorption of the positively charged dye cation because of a reduction in the force of attraction between adsorbent and adsorbate. As it can be seen from the graph PH value of 10 can be considered optimum P^H since percentage removal didn't show any significant increment beyond PH 10. At PH of 10 removal percentage of MB were 91.88%. Similar trends on the effect of initial dye PH were reported by (El-Sayed et al., 2014).

Table 4.11: Effect of PH on MB removal

PH	Absorbance	Ce (mg/l)	Percentage of removal
3	0.171	1.58	84.2
6	0.132	1.22	87.85
9	0.09	0.84	91.3
12	0.086	0.8	92

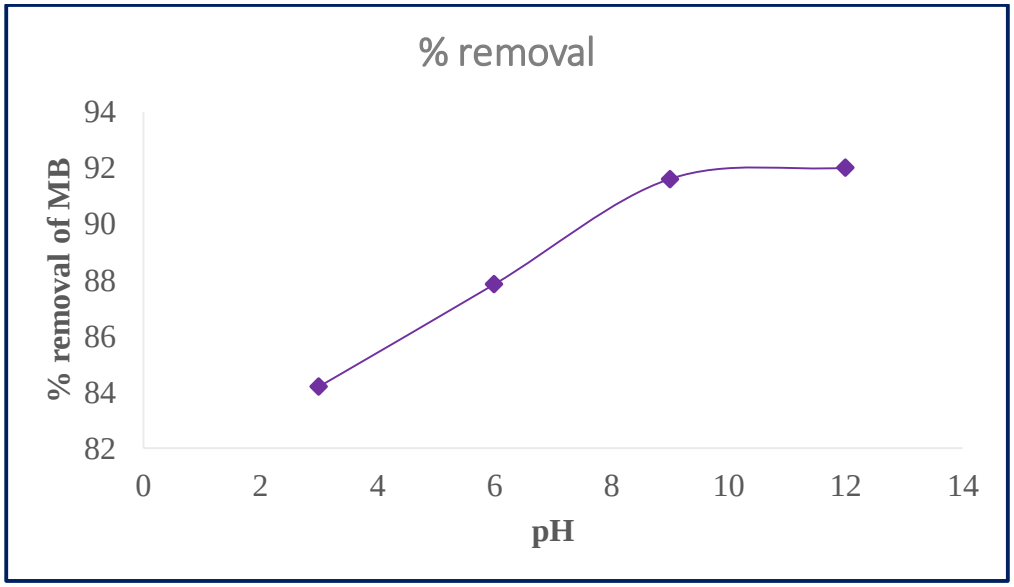

Figure 4.16: Effect of PH on percentage removal of MB at 10mg/l initial concentration, 0.05g adsorbent dosage and contact time of 60min

4.5.2.3 Effect of Contact Time

Results obtained from the investigation of effect of contact time on MB removal are shown in (Fig 4.18). For10 mg/l of MB, 0.05 g of AC and PH of 10 percentage removal of MB increases with increase in contact time. As it can be seen from the figure a rapid rise in the percentage removal were observed with in lower contact time values up to 60min. Thereafter no significant change is observed on the removal percentage of MB dye as contact time varies further to 120 min. at a contact time of 60 min the percentage removal were 93.04 % and at 120 min its value were 93.67% which shows no significant variation between the two. Thus, equilibrium can be assumed after 60min. Therefore 60min were considered as an optimum contact time for conducting the

adsorption experiment in this study. Similar result has been reported by (Rashid et al., 2018) who worked on preparation of Activated Carbon from Coconut Leaves using $FeCl_3$ and Application for Methylene Blue Removal.

Table 4.12**:** Effect of contact time on MB adsorption

Contact time (min)	Absorbance	Ce (mg/l)	Percentage of MB removal
20	0.272	2.52	74.8
40	0.128	1.185	88.15
60	0.078	0.726	93.04
80	0.0697	0.645	93.55
100	0.0686	0.635	93.65
120	0.068	0.633	93.67

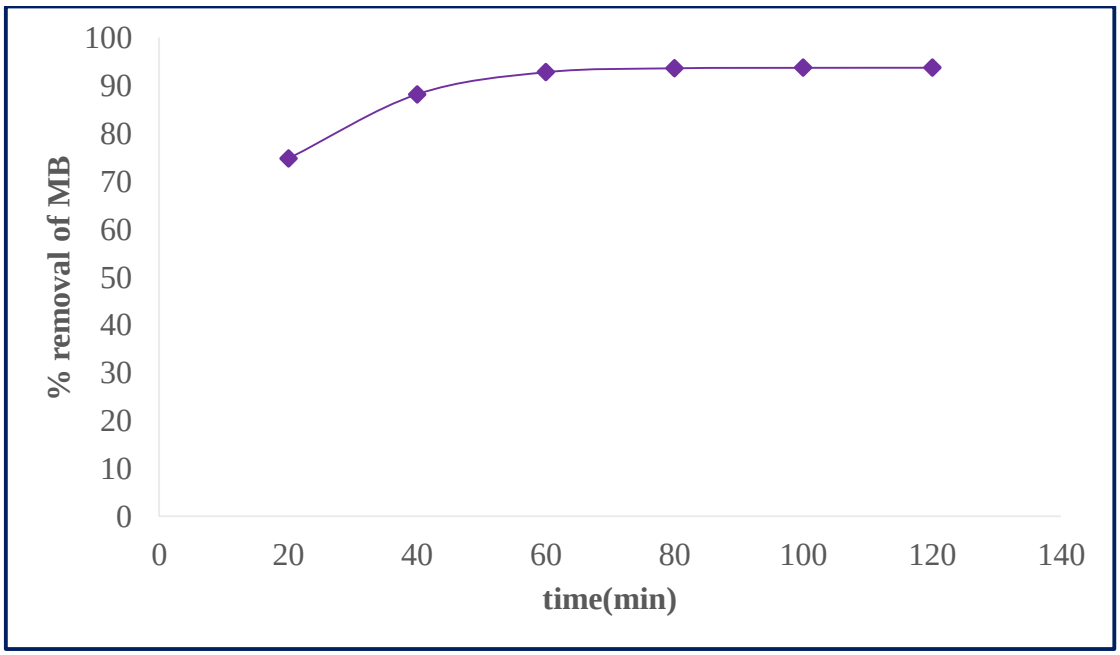

Figure 4.17**:** Effect of contact time on percentage removal of MB adsorption 10mg/l initial concentration, 0.05 g adsorbent dosage and PH 10

4.5.2.4 Effect of Initial Dye Concentration

Initial MB concentration affects the adsorption process due to the fact that dye concentration is dependent on the available binding active sites found on the adsorbent surface. Experiments were conducted at constant adsorption parameters (0.05 g, PH 10 and 60 min) by varying initial dye concentration in the range of (10-50 mg l^{-1}) and Results from the investigation of effect of initial dye concentration on removal percentage are shown in the (Fig 4.19). As it can be observed from the figure it is evident that maximum removal of MB (94.2 %) were achieved at minimum initial concentration of dye (10 mg l^{-1}). Afterwards the removal percentage gradually decrease as initial dye concentration was raised. This might be because of the adsorption sites were fixed and reached saturation. Hence, with increase in initial dye concentration no further adsorption could be achieved so that percentage removal experiences a decrease. Similar trend has been also investigated by (El-Sayed et al., 2014) who worked on Assessment of activated carbon prepared from corncob by chemical activation with phosphoric acid.

Table 4.13**:** Effect of initial concentration on MB adsorption

Initial concentration (mg l^{-1})	Absorbance	Ce (mg l^{-1})	Percentage of MB removal
10	0.063	0.58	94.2
20	0.375	3.474	82.63
30	0.71	6.57	78.10
40	1.23	11.4	71.5
50	1.782	16.5	67.0

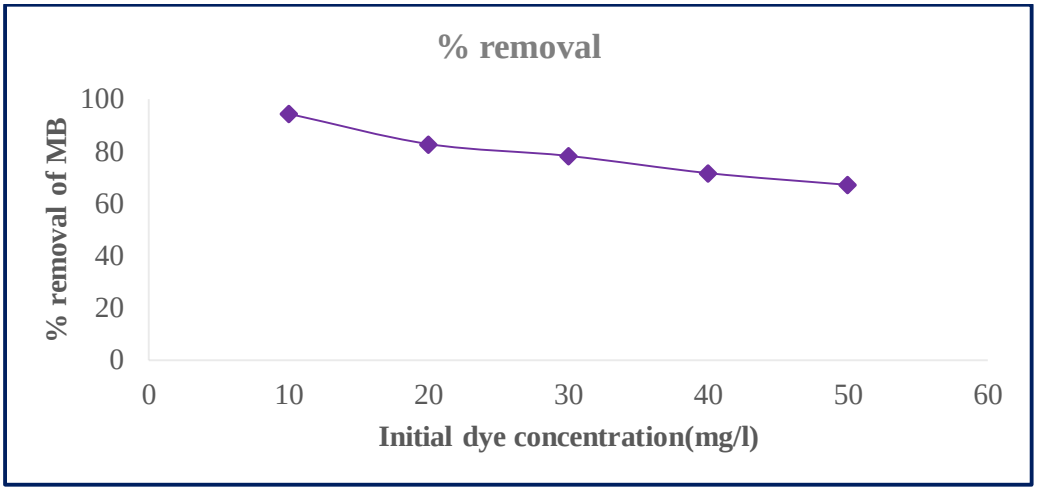

Figure 4.18: Effect of initial dye concentration on percentage removal of MB at 0.05g of adsorbent dosage, PH of 10 and contact time of 60min

4.6 Adsorption Isotherm Study

Adsorption isotherm studies describe the interaction of adsorbate with the adsorbent, and the established equilibrium between adsorbed dye and the residual dye in the solution during the surface adsorption. The interaction between the dye to be adsorbed and adsorbent can be characterized using adsorption isotherm models**.** Adsorption isotherms are mathematical models that describe the distribution of adsorbate species among liquid and adsorbent Based on a set of assumptions that are mainly related to the heterogeneity or homogeneity of adsorbents, type of coverage and possibility of interaction between adsorbate species**.** In this study batch adsorption characteristics of MB removal by FWB activated carbon were studied and the results obtained from the experimentation were used to determine the better isotherm model that the adsorption process follows (Langmuir and/or freundlich).

4.6.1 Langmuir isotherm model

Applicability of Langmuir isotherm model for MB removal was analyzed using the data obtained from batch adsorption experiment by plotting C_e/q_e versus Ce. Fig. 4.19 shows Langmuir plot of MB adsorption at room temperature, PH of 10, adsorbent dosage of 0.05 g, contact time of 60 min and for different initial dye concentrations. The values of Langmuir constants, K_L and q_m were calculated from the intercept and slopes of the linear plot and summarized in (Table 4.15).

Table 4.14: Adsorption of MB using AC derived from FWB at PH of 10, adsorbent dosage of 0.05 g and contact time of 60 min

Initial concentration (mg/l)	C_e (mg/l)	Q_e (mg/g)	lnC_e	$logQ_e$	$logC_e$	C_e/Q_e
10	0.58	18.84	-0.5447	1.275	-0.236	0.031
20	3.474	33.05	1.245	1.519	0.541	0.104
30	6.57	46.86	1.88	1.689	0.818	0.138
40	11.4	57.2	2.433	1.757	1.057	0.1995
50	16.5	67	2.803	1.826	1.217	0.248

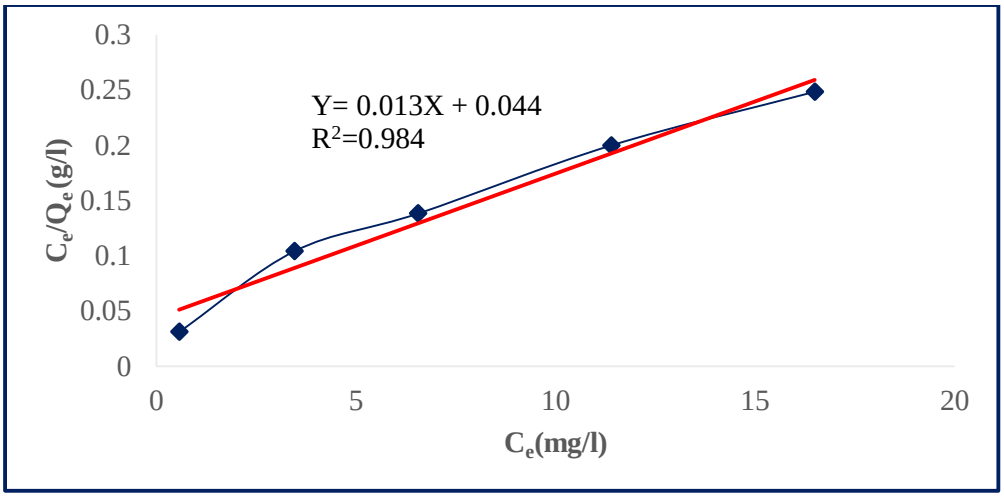

Figure 4.19: langmuir isotherm model for adsorption of MB on FWB based AC at pH 10, time 60min and adsorbent dosage of 0.05g.

4.6.2 Freundlich isotherm model

Results of MB adsorption data were also analyzed according to linear form of freundlich isotherm model were also obtained from adsorption of MB at optimum conditions and results were tabulated in (Table 4.14) and is shown in (Fig. 4.20). Freundlich isotherm constants, K_F and n were determined from slope and intercept of plot of $logC_e$ versus $logq_e$ and are summarized in (Table: 4.15).

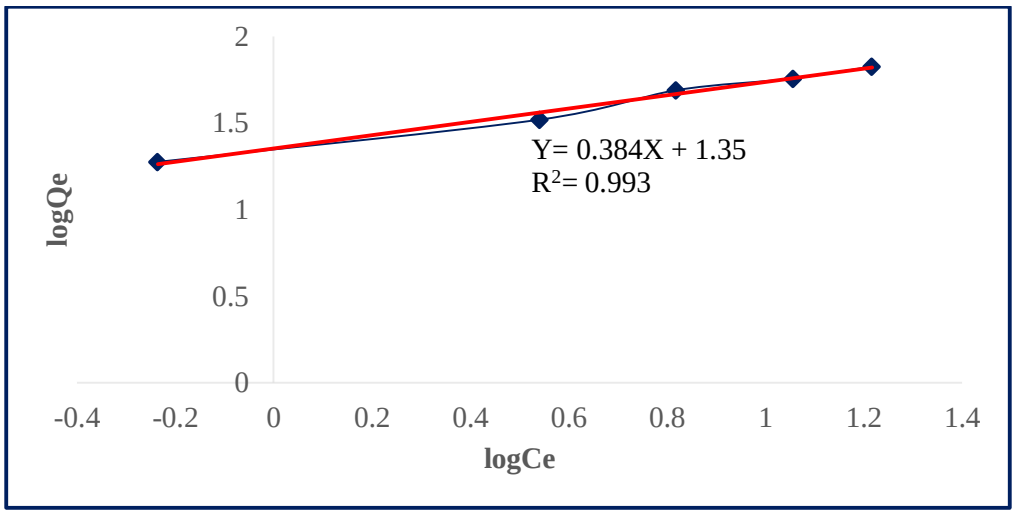

Figure 4.20**:** Friundlich isotherm model for adsorption of MB at pH 10, adsorbent dosage 0.05g and contact time of 60min

4.6.3 Temkin isotherm model

Results of MB adsorption data were obtained from adsorption of MB at optimum conditions and were analyzed according to linear form of Temkin isotherm model and results were tabulated in (Table 4.14) and is shown in (Fig. 4.21). Temkin isotherm constants, K_F and n were determined from slope and intercept of plot of q_e versus lnC_e and are summarized in (Table: 4.15).

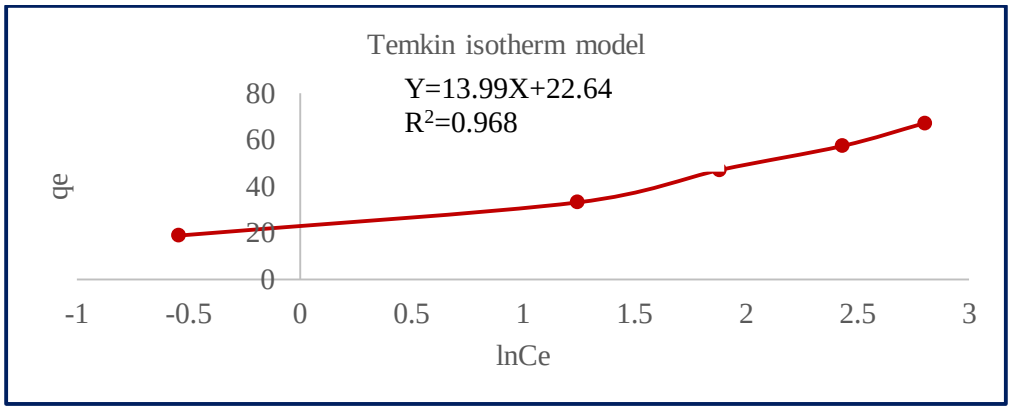

Figure 4.21: Temkin isotherm model for adsorption of MB at pH 10, adsorbent dosage 0.05 g and contact time of 60 min

Table 4.15: Adsorption isotherm model parameters and coefficient of regression, R^2 for MB removal using FWB based activated carbon

Isotherm model	Langmuir model			Frendlich model				Temkin model		
Parameters	q_m (mg/g)	K_L (L/mg)	R^2	R_L	K_f [(mg/g) $(Lmg^{-1})^{1/n}$]	n_f	R^2	β	K_T	R^2
Value	76.92	0.295	0.984	0.33	22.39	2.604	0.993	13.99	5.04	0.968

It can be observed from Fig. 4.19, 4.20 and Fig: 4.21 that adsorption capacity of the AC increases progressively as with increasing in equilibrium concentration of MB. This could be due to the increase in driving force, concentration gradient which accelerated the diffusion of dye molecule on to the surface of ACs (Tian et al., 2019). Isotherm parameters for each respective models summarized in Table (4.15) showed almost higher correlation coefficient approached to unity, (R^2=0.993) were obtained for Freundlich isotherm model, (R^2=0.984) for Langmuir isotherm model and (R^2=0.968) which suggests that the adsorption of MB on the AC better fits with both models but, relatively Freundlich model had a little higher R^2 and it manifested that the adsorption process could be due to multilayer adsorption manner on heterogeneous surface of the adsorbent.

4.7 Adsorption kinetics

Kinetics models (pseudo-first order and pseudo-second order) were investigated at optimum conditions (adsorbent dosage of 0.05g, initial dye concentration of 10 mg/l and PH of 10) for studying the kinetics of the adsorption of methylene blue on flower waste biomass derived activated carbon. Both kinetics models were based on the assumption that the rate of occupation of sorption sites is proportional to the number of unoccupied sites.

4.7.1 Pseudo-first order kinetics model

Experimental results obtained from batch adsorption of MB were analyzed to check the capability of pseudo-first order kinetic model and its respective adsorption model parameters were determined from slope and intercept of linear plot of log (q_e-q_t) versus time as shown in (Fig. 4.22). Values of pseudo-first order kinetic model constants are summarized in (Table: 4.18).

Table 4.16: Experimental results of MB adsorption

Time (min)	C_e (mg/l)	q_t (mg/l)	q_e (mg/l)	Log ($q_e - q_t$)	t/q_t (min/mg.g^{-1})
20	2.52	14.96	18.84	0.589	1.34
40	1.185	17.63	18.84	0.093	2.27
60	0.726	18.55	18.84	-0.538	3.23
80	0.645	18.71	18.84	-0.886	4.28
100	0.635	18.73	18.84	-0.959	5.34
120	0.633	18.734	18.84	-0.975	6.41

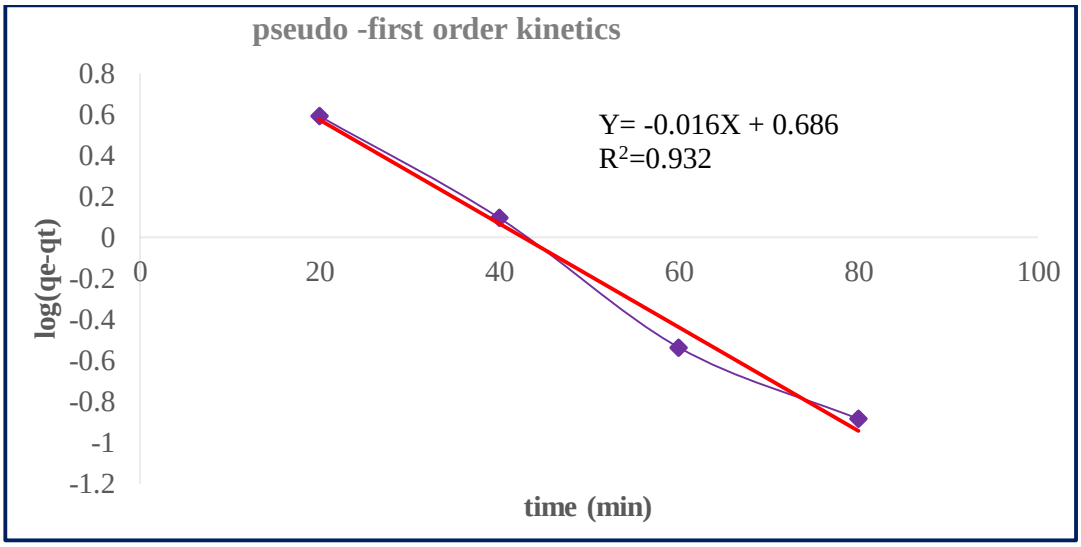

Figure 4.22: linear plots of log (qe-qt) versus t at initial dye concentration of 10 mg/l, 0.05g dosage and PH 10

4.7.2 Pseudo-second order kinetic model

Pseudo-second order kinetic model parameters, K_2 (second order rate constant) and equilibrium concentration of MB q_e were determined from slope and intercept of the corresponding linear plot of t/qt versus time as shown in (Fig: 4.23) and the values for those parameters are summarized in (Table: 4.18)

Table 4.17: Experimental results of MB adsorption

T (min)	Ce (mgl^{-1})	q_e (mgl^{-1})	q_t (mgl^{-1})	t/q_t ($min/mg.g^{-1}$)
20	2.52	18.84	14.96	1.34
40	1.185	18.84	17.63	2.27
60	0.726	18.84	18.55	3.23
80	0.645	18.84	18.71	4.28
100	0.635	18.84	18.73	5.34
120	0.633	18.84	18.734	6.41

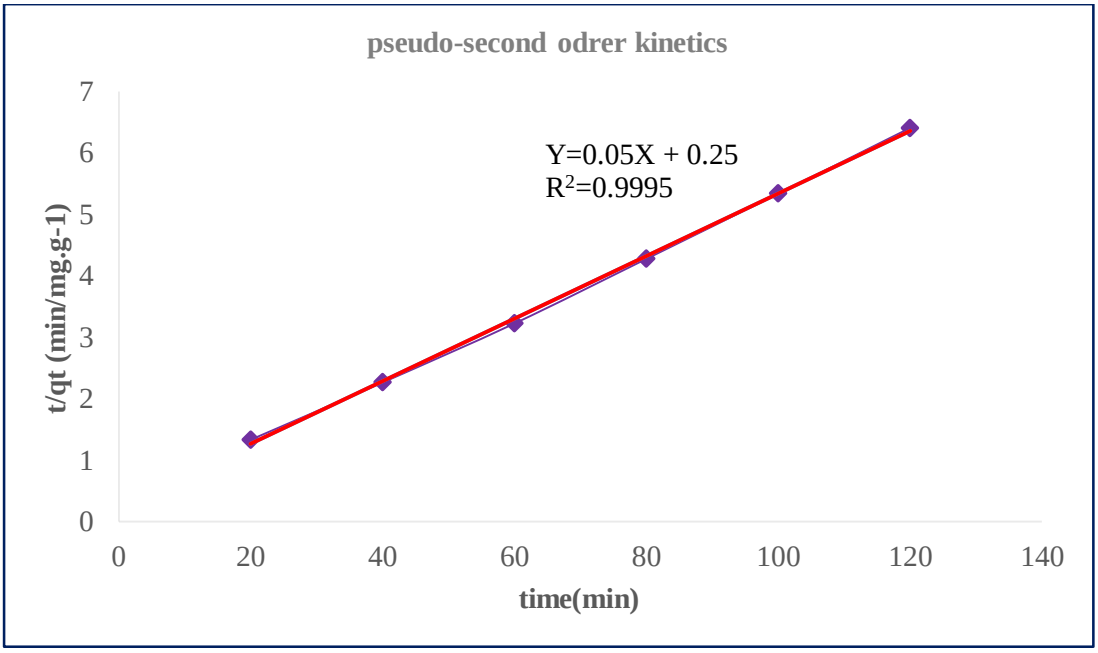

Figure 4.23: linear plot of t versus t/qt for MB removal at initial dye concentration of 10 mg l^{-1}, dosage of 0.05 g and PH of 10

Table 4.18: Kinetics Model Parameters and Correlation Coefficient for MB Adsorption using FWB based AC at optimum conditions

Kinetic model	Pseudo-first order model			Pseudo-second order model		
Parameters	$K_1(min^{-1})$	q_e (mg/g)	R^2	K_2 (g.mg^{-1}. min)	q_e (mg/g)	R^2
Values	$6.95*10^{-3}$	4.853	0.932	0.01	20	0.9995

According to the values of correlation coefficient, R^2 obtained (see Table 4.18), Fitting of adsorption experimental data using pseudo-second order model showed a higher (R^2 =0.995) value which showed that the kinetics of adsorption of MB could be better described by pseudo-second order model. It can be noted that rate of the adsorption of MB appears be controlled by the chemical reaction. Similar elaboration has been justified by (Tian et al., 2019) as if the adsorption kinetics on the ACs could be described by a pseudo-second-order model, it indicates that the adsorption rate might be largely controlled by a chemisorption process.

4.8 Effect of activation temperature on removal efficiency of MB using FWB derived activated carbon at optimum adsorption condition

Table 4.19 : Effect of activation temperature on MB removal efficiency of AC from FWB

Temperature (^{o}C)	AC sample	Removal efficiency (%)
400	AC-1.541	68.04
500	AC-151	94.2
600	AC-1.561	72.53

At optimized condition of adsorption process (PH of 10, adsorbent dosage of 0.05g, initial dye concentration of 10 mg.l^{-1} and contact time of 60min.) three activated carbon samples produced at different activation temperature were selected and tested for removal efficiency of MB at the same conditions and results in (Table: 4.19) showed that AC produced at adsorption using AC at 500^{o}C had maximum removal efficiency as compared with the others.

4.9 Comparison to other activated carbons

Surface area and other adsorptive characteristics of AC from the present study were compared with other ACs from previous studies as indicated in (Table: 4.20). Maximum surface area of AC produced from flower waste biomass were 750 m^2 g^{-1}. This value is comparable to surface area of ACs produced through physical activation as well as chemical activation. However, significant difference to some of the ACs in the literatures is due to the difference in precursor and width of experimentation domain that has been used during the time of preparation synthesis conditions.

Table: 4.20 Comparison of textural characteristics of AC from FWB with other ACs reported in the literature

Raw material	Activating agent	BET Surface area	Remark	Reference
FWB	$ZnCl_2$ (1:1 and 500 ^oC)	750	Mild condition	This study
Tomato stem	$ZnCl_2$ (2.5:1 and 700^oC)	971	Higher activating agent and temperature	(Fu et al., 2017)
Barley husks	$ZnCl_2$ (1:1 and 436 ^oC)	811.4	Comparable	(Loredo-Cancino et al., n.d.)
Pineapple waste biomass	$ZnCl_2$, (1:1 and 500^oC)	914.7	Comparable	(Mahamad et al., 2015)
Babassu nutshell	CO_2 (700 ^oC)	543.5	Lower surface area	(Salgado et al., 2018)
Textile sewage sludges	KOH (700 ^oC)	311.62	Lower surface area	(Kacan, 2016)

5 CONCLUSION AND RECOMMENDATION

5.1 Conclusion

This study has investigated the preparation and characterization of AC from FWB by chemical activation using $ZnCl_2$ and its application for MB removal. The experimental results showed that, FWB can be used to prepare AC and BET surface area of the produced AC were influenced by impregnation ratio, carbonization temperature, and carbonization time. BET surface area were increased with impregnation ratio up to 1:1 and then decreased. Activation temperature from 400 to 500 ^oC and activation time from 30 to 60min resulted in increased BET surface area. Extended activation at higher temperature beyond 500 ^oC and activation period above 60min lead to minimum surface area of AC. AC obtained at Preparation conditions (I.R 1:1, carbonization temperature 500 ^oC and activation time 1hr) has a maximum surface area of 750 $m^2 g^{-1}$.

Surface morphology of AC was analyzed by SEM and elemental composition of AC were analyzed by EDS. SEM image of the activated carbon showed irregular slit structure micrograph which support the formation well developed pores on the AC surface. BET Surface area and average pore diameter of activated carbons were determined by N_2 adsorption – desorption. BET surface area, pore volume and mean pore diameter were 750 $m^2 g^{-1}$, 1.91 cm^{-1} and 1.89 nm respectively. The EDS analysis confirmed the presence of different elements and the AC structure were mostly contained by carbon atom (87.97% and trace amounts of nitrogen, oxygen, sulfur, chlorine and zinc. As compared to the carbon content of FWB (49.57%) AC have increased carbon content (87.97%) which is resulted from activation using $ZnCl_2$.

Adsorption capacity of the FWB derived AC were tested by MB adsorption through batch adsorption technique at different adsorption conditions. The various adsorption parameters such as effect of initial dye concentration, pH, contact time, and adsorbent dose on the adsorption of the MB were studied and the results showed that, best conditions for adsorption of MB on to FWB derived AC were found to be solution PH of 10, adsorbent dosage of 0.05g, initial MB concentration of 10 $mg.l^{-1}$ and contact time of 60 min. The adsorption equilibrium data was analyzed by Langmuir, Freundlich and Temkin adsorption isotherms. Also, adsorption kinetics data was evaluated by pseudo first order and pseudo second order kinetics. Accordingly, the isotherm were best fitted with both Freundlich (0.993) and Langmuir isotherm (0.984) model and

the mechanism obeys pseudo-second order kinetic model with R^2 value of 0.987. Based on Freundlich model maximum removal efficiency of 94% was obtained at room temperature, Adsorption study showed that FWB based AC can be effectively used for removal of pollutants from wastewater streams due to the presence of binding active sites. Thus, FWB is a potential raw material for AC production and using FWB precursor can significantly reduce waste biomass disposal to the environment.

5.2 Recommendation

Due to wide application of dyes in different socio-economic activities, treatment of industrial wastewater effluents need greater attention. In this study AC were prepared from FWB via chemical activation using $ZnCl_2$. However, the potential of FWB as a precursor for AC production can be supported by further researches using different activating agents such as sulfuric acid, potassium hydroxide, sodium hydroxide and potassium carbonate so that surface properties of AC could be improved. Flower mixed with stem were used as a raw material, however, the difference in BET surface area should be tested by further investigation using flower, stem and leaves separately. The produced AC in this study was tested only for MB removal. Thus, it is recommended to test its performance as an adsorbent for other pollutants such as pesticide based wastes, so that, it might be possible to use FWB derived AC to treat floriculture industries wastewater stream. MB Adsorption in this study were done using synthetic wastewater sample at room temperature, so it is recommended to further study the adsorption using real industrial or municipal wastewater at varied adsorption temperature. The feasibility of AC production could be investigated by studying the amount of FWB generated at every flower grower industries in the country.

6 REFERENCE

[1] Abbasi, H., & Asgari, H. (2018). Removal of methylene blue from aqueous solutions using luffa adsorbent modified with sodium dodecyl sulfate anionic surfactant. Global Nest Journal, 20(3), 582–588. Https://doi.org/10.30955/gnj.002722

[2] Abdulsalam, J., Mulopo, J., Oboirien, B., Bada, S., & Falcon, R. (2019). Experimental evaluation of activated carbon derived from South Africa discard coal for natural gas storage. International Journal of Coal Science & Technology, 6(3), 459–477. Https://doi.org/10.1007/s40789-019-0262-5

[3] Ahiduzzaman, M. (2016). Evaluation of Characteristics of Activated Carbon from Rice Husk Impregnated with Zinc Chloride and Phosphoric Acid. American Journal of Physical Chemistry, 5(5), 94. Https://doi.org/10.11648/j.ajpc.20160505.12

[4] Ahmad, A. L., Loh, M. M., & Aziz, J. A. (2007). Preparation and characterization of activated carbon from oil palm wood and its evaluation on Methylene blue adsorption. Dyes and Pigments, 75(2), 263–272. Https://doi.org/10.1016/j.dyepig.2006.05.034

[5] Alhamed, Y. (2006). Activated Carbon from Dates' Stone by zncl2 Activation. Journal of King Abdulaziz University-Engineering Sciences, 17(2), 75–98. Https://doi.org/10.4197/Eng.17-2.4

[6] Baseri, J. R., Palanisamy, P. N., & Sivakumar, P. (2012). Preparation and characterization of activated carbon from Thevetia peruviana for the removal of dyes from textile waste water. Advances in Applied Science Research, 3(1), 377–383. Retrieved from www.pelagiaresearchlibrary.com

[7] Basta, A. H., Fierro, V., El-Saied, H., & Celzard, A. (2009). 2-Steps KOH activation of rice straw: An efficient method for preparing high-performance activated carbons. Bioresource Technology, 100(17), 3941–3947. Https://doi.org/10.1016/j.biortech.2009.02.028

[8] Bedmohata MA, Chaudhari AR, Singh SP, & Choudhary. (2015). Adsorption Capacity of Activated Carbon Prepared by Chemical Activation of Lignin for the Removal of Methylene Blue Dye. International Journal of Advanced Research in Chemical Science (IJARCS), 2(8), 1–13. Retrieved from www.arcjournals.org

[9] Berrios, M., Martín, M. Ángeles, & Martín, A. (2012). Treatment of pollutants in

wastewater: Adsorption of methylene blue onto olive-based activated carbon. Journal of Industrial and Engineering Chemistry, 18(2), 780–784. Https://doi.org/10.1016/j.jiec.2011.11.125

[10] Caturla, F., Molina-Sabio, M., & Rodríguez-Reinoso, F. (1991). Preparation of activated carbon by chemical activation with ZnCl2. Carbon, 29(7), 999–1007. https://doi.org/10.1016/0008-6223(91)90179-M

[11] Chang, J., Gao, Z., Wang, X., Wu, D., Xu, F., Wang, X., … Jiang, K. (2015). Activated porous carbon prepared from paulownia flower for high performance supercapacitor electrodes. Electrochimica Acta, 157, 290–298. https://doi.org/10.1016/j.electacta.2014.12.169

[12] Chincholi M., Sagwekar P., Nagaria C., K. S. & D. S. (2014). Removal of dye by adsorption on various adsorbents : A review. International Journal of Science, Engineering and Technology Research (IJSETR), 3(4), 835–840.

[13] Choerospondias, L., & Shrestha, R. M. (2015). By. (Ii).

[14] Corda, N. C., & Kini, M. S. (2018). A Review on Adsorption of Cationic Dyes using Activated Carbon. MATEC Web of Conferences, 144, 1–16. https://doi.org/10.1051/matecconf/201714402022

[15] Deng, H., Yang, L., Tao, G., & Dai, J. (2009). Preparation and characterization of activated carbon from cotton stalk by microwave assisted chemical activation-Application in methylene blue adsorption from aqueous solution. Journal of Hazardous Materials, 166(2–3), 1514–1521. https://doi.org/10.1016/j.jhazmat.2008.12.080

[16] El-Sayed, G. O., Yehia, M. M., & Asaad, A. A. (2014). Assessment of activated carbon prepared from corncob by chemical activation with phosphoric acid. Water Resources and Industry, 7–8, 66–75. https://doi.org/10.1016/j.wri.2014.10.001

[17] Engineering, B. (2016). Addis Ababa Institute of Technology School of Chemical and Bio Engineering Removal of Lead From Waste Water Using Corn Cob Activated Carbon As an Adsorbent.

[18] Fu, K., Yue, Q., Gao, B., Wang, Y., & Li, Q. (2017). Activated carbon from tomato stem by chemical activation with FeCl 2. Colloids and Surfaces A: Physicochemical and Engineering Aspects, 529, 842–849. https://doi.org/10.1016/j.colsurfa.2017.06.064

[19] Gonawala, K. H., & Mehta, M. J. (2014). Removal of Color from Different Dye Wastewater by Using Ferric Oxide as an Adsorbent. Int. Journal of Engineering Research and Applications, 4(5), 102–109.

[20] González-García, P. (2018). Activated carbon from lignocellulosics precursors: A review of the synthesis methods, characterization techniques and applications. Renewable and Sustainable Energy Reviews, 82(August 2017), 1393–1414. https://doi.org/10.1016/j.rser.2017.04.117

[21] Guo, J., Song, Y., Ji, X., Ji, L., Cai, L., Wang, Y., … Song, W. (2019). Preparation and characterization of nanoporous activated carbon derived from prawn shell and its application for removal of heavy metal ions. Materials, 12(2). https://doi.org/10.3390/ma12020241

[22] Gurten, I. I., Ozmak, M., Yagmur, E., & Aktas, Z. (2012). Preparation and characterisation of activated carbon from waste tea using K 2CO 3. Biomass and Bioenergy, 37, 73–81. https://doi.org/10.1016/j.biombioe.2011.12.030

[23] Hu, Z., Srinivasan, M. P., & Ni, Y. (2001). Novel activation process for preparing highly microporous and mesoporous activated carbons. Carbon, 39(6), 877–886. https://doi.org/10.1016/S0008-6223(00)00198-6

[24] In, t., & tilahun advisor, -abayneh. (2013). Environmental impacts of floriculture industry in debrezeit town: a need for strategic environmental assessment environmental planning and landscape design graduate study in environmental planning and landscape design faculty of technology-eiabc addis ababa university., addis abeba. (july).

[25] Ioannidou, O., & Zabaniotou, A. (2007). Agricultural residues as precursors for activated carbon production-A review. Renewable and Sustainable Energy Reviews, 11(9), 1966–2005. https://doi.org/10.1016/j.rser.2006.03.013

[26] Joshi, R. R. (2016). Optimization of Conditions for the Preparation of Activated Carbon from Lapsi (Choerospondias axillaris) Seed Stone Using $ZnCl_2$. Journal of the Institute of Engineering, 11(1), 128–139. https://doi.org/10.3126/jie.v11i1.14707

[27] Kacan, E. (2016). Optimum BET surface areas for activated carbon produced from textile sewage sludges and its application as dye removal. Journal of Environmental Management, 166, 116–123. https://doi.org/10.1016/j.jenvman.2015.09.044

[28] Kassa, M. (2017). Review on Environmental Effects of Ethiopian Floriculture Industry. Asian Research Journal of Agriculture, 4(2), 1–13. https://doi.org/10.9734/arja/2017/31884

[29] Khaled, A., Nemr, A. El, El-Sikaily, A., & Abdelwahab, O. (2009). Removal of Direct N Blue-106 from artificial textile dye effluent using activated carbon from orange peel: Adsorption isotherm and kinetic studies. Journal of Hazardous Materials, 165(1–3), 100–110. https://doi.org/10.1016/j.jhazmat.2008.09.122

[30] Kumar, A., & Jena, H. M. (2015). High surface area microporous activated carbons prepared from Fox nut (Euryale ferox) shell by zinc chloride activation. Applied Surface Science, 356, 753–761. https://doi.org/10.1016/j.apsusc.2015.08.074

[31] Liu, R. L., Liu, Y., Zhou, X. Y., Zhang, Z. Q., Zhang, J., & Dang, F. Q. (2014). Biomass-derived highly porous functional carbon fabricated by using a free-standing template for efficient removal of methylene blue. Bioresource Technology, 154, 138–147. https://doi.org/10.1016/j.biortech.2013.12.034

[32] Loredo-Cancino, M., … E. S.-R.-J. of environmental, & 2013, undefined. (n.d.). Determining optimal conditions to produce activated carbon from barley husks using single or dual optimization. Elsevier. Retrieved from https://www.sciencedirect.com/science/article/pii/S0301479713002004

[33] M.A. Tadda, A. Ahsan, A. Shitu, M. ElSergany, T. Arunkumar, Bipin Jose, M. Abdur Razzaque, N. N. N. D., Tadda, M. A., Ahsan, A., Shitu, A., ElSergany, M., Arunkumar, T., … Daud, N. N. N. (2016). A review on activated carbon: process, application and prospects. Journal of Advanced Civil Engineering Practice and Research, 2(1), 7–13. https://doi.org/10.1016/B978-1-59-749641-4.00015-1

[34] Ma, X., Zhang, F., Zhu, J., Yu, L., & Liu, X. (2014). Preparation of highly developed mesoporous activated carbon fiber from liquefied wood using wood charcoal as additive and its adsorption of methylene blue from solution. Bioresource Technology, 164, 1–6. https://doi.org/10.1016/j.biortech.2014.04.050

[35] Mahamad, M. N., Zaini, M. A. A., & Zakaria, Z. A. (2015). Preparation and characterization of activated carbon from pineapple waste biomass for dye removal. International Biodeterioration and Biodegradation, 102, 274–280.

https://doi.org/10.1016/j.ibiod.2015.03.009

[36] Mui, E. L. K., Cheung, W. H., Valix, M., & Mckay, G. (2010). Activated carbons from bamboo scaffolding using acid activation. Separation and Purification Technology, 74(2), 213–218. https://doi.org/10.1016/j.seppur.2010.06.007

[37] Oliveira, L. C. A., Pereira, E., Guimaraes, I. R., Vallone, A., Pereira, M., Mesquita, J. P., & Sapag, K. (2009). Preparation of activated carbons from coffee husks utilizing FeCl3 and ZnCl2 as activating agents. Journal of Hazardous Materials, 165(1–3), 87–94. https://doi.org/10.1016/j.jhazmat.2008.09.064

[38] On, P. R. (n.d.). <Production and characterization of Activated carbon rice husk.pdf>.

[39] Ozdemir, I., Şahin, M., Orhan, R., & Erdem, M. (2014). Preparation and characterization of activated carbon from grape stalk by zinc chloride activation. Fuel Processing Technology, 125, 200–206. https://doi.org/10.1016/j.fuproc.2014.04.002

[40] Paraskeva, P., Kalderis, D., & Diamadopoulos, E. (2008). Production of activated carbon from agricultural by-products. 592(May 2007), 581–592. https://doi.org/10.1002/jctb

[41] Pereira, R. G., Veloso, C. M., Da Silva, N. M., De Sousa, L. F., Bonomo, R. C. F., De Souza, A. O., … Da Costa Ilhéu Fontan, R. (2014). Preparation of activated carbons from cocoa shells and siriguela seeds using H3PO4 and ZnCL2 as activating agents for BSA and α-lactalbumin adsorption. Fuel Processing Technology, 126, 476–486. https://doi.org/10.1016/j.fuproc.2014.06.001

[42] Rashid, R. A., Jawad, A. H., Ishak, M. A. B. M., & Kasim, N. N. (2018). FeCl 3 - activated carbon developed from coconut leaves: Characterization and application for methylene blue removal. Sains Malaysiana, 47(3), 603–610. https://doi.org/10.17576/jsm-2018-4703-22

[43] Rezma, S., Birot, M., Hafiane, A., & Deleuze, H. (2017). Préparation de charbons actifs microporeux à partir d'une nouvelle matière première issue de la biomasse : les pétioles de palmiers dattiers. Comptes Rendus Chimie, 20(9–10), 881–887. https://doi.org/10.1016/j.crci.2017.05.003

[44] Rodrigues, L. A., da Silva, M. L. C. P., Alvarez-Mendes, M. O., Coutinho, A. dos

R., & Thim, G. P. (2011). Phenol removal from aqueous solution by activated carbon produced from avocado kernel seeds. Chemical Engineering Journal, 174(1), 49–57. https://doi.org/10.1016/j.cej.2011.08.027

[45] Saad, M. J., Chia, C. H., Zakaria, S., Sajab, M. S., Misran, S., Rahman, M. H. A., & Chin, S. X. (2019). Physical and chemical properties of the rice straw activated carbon produced from carbonization and KOH activation processes. Sains Malaysiana, 48(2), 385–391. https://doi.org/10.17576/jsm-2019-4802-16

[46] Sahira, J., Mandira, A., Prasad, P. B., & Ram, P. R. (2013). Effects of Activating Agents on the Activated Carbons Prepared from Lapsi Seed Stone. Research Journal of Chemical Science, 3(5), 19–24.

[47] Salgado, M. D. F., Abioye, A. M., Junoh, M. M., Santos, J. A. P., & Ani, F. N. (2018). Preparation of activated carbon from babassu endocarpunder microwave radiation by physical activation. IOP Conference Series: Earth and Environmental Science, 105(1). https://doi.org/10.1088/1755-1315/105/1/012116

[48] Sayğılı, H., & Güzel, F. (2018). Novel and sustainable precursor for high-quality activated carbon preparation by conventional pyrolysis: Optimization of produce conditions and feasibility in adsorption studies. Advanced Powder Technology, 29(3), 726–736. https://doi.org/10.1016/j.apt.2017.12.014

[49] Sayılı, H., Güzel, F., & Önal, Y. (2015). Conversion of grape industrial processing waste to activated carbon sorbent and its performance in cationic and anionic dyes adsorption. Journal of Cleaner Production, 93, 84–93. https://doi.org/10.1016/j.jclepro.2015.01.009

[50] Schröder, E., Thomauske, K., Weber, C., Hornung, A., & Tumiatti, V. (2007). Experiments on the generation of activated carbon from biomass. Journal of Analytical and Applied Pyrolysis, 79(1-2 SPEC. ISS.), 106–111. https://doi.org/10.1016/j.jaap.2006.10.015

[51] Selvaraju, G., & Bakar, N. K. A. (2017). Production of a new industrially viable green-activated carbon from Artocarpus integer fruit processing waste and evaluation of its chemical, morphological and adsorption properties. Journal of Cleaner Production, 141, 989–999. https://doi.org/10.1016/j.jclepro.2016.09.056

[52] Şentorun-Shalaby, Ç., Uçak-Astarlioğlu, M. G., Artok, L., & Sarici, Ç. (2006). Preparation and characterization of activated carbons by one-step steam pyrolysis/activation from apricot stones. Microporous and Mesoporous Materials, 88(1–3), 126–134. https://doi.org/10.1016/j.micromeso.2005.09.003

[53] Singh, K., Kumar, P., & Srivastava, R. (2017). An overview of textile dyes and their removal techniques: Indian perspective. Pollution Research, 36(4), 790–797.

[54] Sivaraj, R., Rajendran, V., & Gunalan, G. S. (2010). Preparation and characterization of activated carbons from parthenium biomass by physical and chemical activation techniques. E-Journal of Chemistry, 7(4), 1314–1319. https://doi.org/10.1155/2010/948015

[55] Tian, D., Xu, Z., Zhang, D., Chen, W., Cai, J., Deng, H., … Zhou, Y. (2019). Micro–mesoporous carbon from cotton waste activated by FeCl3/ZnCl2: Preparation, optimization, characterization and adsorption of methylene blue and eriochrome black T. Journal of Solid State Chemistry, 269(October 2018), 580–587. https://doi.org/10.1016/j.jssc.2018.10.035

[56] Tongpoothorn, W., Sriuttha, M., Homchan, P., Chanthai, S., & Ruangviriyachai, C. (2011). Preparation of activated carbon derived from Jatropha curcas fruit shell by simple thermo-chemical activation and characterization of their physico-chemical properties. Chemical Engineering Research and Design, 89(3), 335–340. https://doi.org/10.1016/j.cherd.2010.06.012

[57] Varil, T., Bergna, D., Lahti, R., Romar, H., Hu, T., & Lassi, U. (2017). Activated carbon production from peat using ZnCl2: Characterization and applications. BioResources, 12(4), 8078–8092. https://doi.org/10.15376/biores.12.4.8078-8092

[58] Zhang, S., Tao, L., Jiang, M., Gou, G., & Zhou, Z. (2015). Single-step synthesis of magnetic activated carbon from peanut shell. Materials Letters, 157, 281–284. https://doi.org/10.1016/j.matlet.2015.05.117